Beneficial effects of commensal microbes against enteric infection and inflammatory bowel disease

Jin Sun You

Department of Medical Science

The Graduate School, Yonsei University

Beneficial effects of commensal microbes against enteric infection and inflammatory bowel disease

Directed by Professor Sang Sun Yoon

The Doctoral Dissertation
submitted to the Department of Medical Science,
the Graduate School of Yonsei University
in partial fulfillment of the requirements for the degree
of Doctor of Philosophy

Jin Sun You

December 2022

This certifies that the Doctoral
Dissertation of Jin Sun You
is approved.

Thesis Supervisor : Sang Sun Yoon

Thesis Committee Member#1 : Ki Taek Nam

Thesis Committee Member#2 : Dong Eun Yong

Thesis Committee Member#3 : Byung Yong Kim

Thesis Committee Member#4 : Jae Hee Cheon

The Graduate School
Yonsei University

December 2022

ACKNOWLEDGEMENTS

학위 과정을 마치며 지난 시간을 돌아보니 참 많은 일도 있었고, 또 그 과정에서 많은 것을 배우게 된 값진 시간들이었습니다. 먼저, 지난 6년이라는 시간동안 여기까지 올 수 있게 이끌어 주시고 응원해 주신 윤상선 교수님께 감사의 말씀을 올립니다. 혼자서는 절대 올 수 없었던 길이었지만, 교수님께서 이끌어 주시고 길을 알려주셨기에 여기까지 올 수 있었던 여정이었다고 생각합니다. 교수님의 제자라는 것이 늘 자랑스러웠으며 항상 든든했습니다. 이런 생각을 가지고 학위과정을 할 수 있도록 도와주신 윤상선 교수님께 진심으로 감사의 말씀을 드립니다.

갑작스러운 코로나 시국으로 인하여 바쁘신 일정 중에서도 시간을 내주셔서 저의 학위과정을 지켜봐 주신 남기택 교수님, 용동은 교수님, 김병용 박사님, 천재희 교수님께 진심으로 감사의 말씀을 올립니다. 저의 연구에 관심을 가지고 조언해 주시고, 또한 제가 진정한 과학자가 될 수 있도록 도와주셔서 정말 감사드리며, 그 덕분에 이렇게 학위과정을 잘 마무리 할 수 있었습니다. 감사드립니다.

2017년 1월에 실험실에 들어와서 지금까지, 길다면 길고 짧다면 짧은 시간동안 저와 함께 해준 우리 실험실 식구들 정말 고맙습니다. 실험실 생활을 하면서 힘들 수도 있었던 시간들, 우리 실험실 식구들 덕분에 무탈하게 잘 넘기고 이렇게 학위과정을 잘 마무리 할 수 있게 되었습니다. 먼저 많은 도움을 주셨던 윤미영 박사님, 이강무 박사님, 김지은

박사님께 진심으로 감사의 말씀을 드립니다. 처음 실험실에 들어왔을 때 함께했던 동근이, 기훈쌤에게도 고맙단 말씀을 전합니다. 학위 과정의 많은 시간을 함께하고 도와줬던 화영이, Mohammed, 원태, 경배쌤, 태강쌤, 다현이, 지현이 모두들 하시는 일 잘 되시길 바라며 그동안 많이 감사하였습니다. 실험하면서 많은 것을 같이 함께한 광희쌤, 유진이, 그동안 함께 해 주셔서 감사합니다. 늘 긍정적인 에너지를 주셨던 찬민쌤, 소원쌤, 윤이쌤 그동안 감사했습니다. 그리고 실험실 생활의 많은 부분에서 잘 챙겨주고 실험실 살림이 잘 돌아갈 수 있도록 도와주고 힘이 되어 주는 우리 후배들, 경진이, 채영이, 지원이, 윤지, 준범이, 모두들 고맙습니다.

마지막으로 부모님께 감사의 말씀을 전합니다. 애교도 없고 무뚝뚝한 철없는 딸, 실험이 늦게 끝나면 귀갓길이 걱정되어 데리러 와 주시고, 학회 갔다 오는 날이면 짐 무거울까 걱정되어 마중 나와 주시는 부모님. 늘 제 뒤에서 물심양면으로 도와주시고 응원해 주셔서 진심으로 감사드립니다. 더 멋진 사람이 되어서 주신 사랑에 보답할 수 있도록 노력하겠습니다. 진심으로 감사드립니다.

좋은 분들과 함께 할 수 있어서 즐겁고 행복하게 학위 과정을 할 수 있었습니다. 긴 여정동안 함께 해주시고 도움을 주신 모든 분들께 감사의 말씀을 전합니다. 감사드립니다.

유진선 드림

<TABLE OF CONTENTS>

LIST OF FIGURES

LIST OF TABLES

ABSTRACT

Beneficial effects of commensal microbes
against enteric infection and
inflammatory bowel disease

Jin Sun You

Department of Medical Science
The Graduate School, Yonsei University

Directed by Professor Sang Sun Yoon

Gut microbiota is closely related to the health status of the host. Maintaining the balance of intestinal microflora plays a crucial role in maintaining the healthy state of the host. When the balance of these intestinal microflora is disrupted, it is called dysbiosis.
In the dysbiosis state, the intestinal microflora becomes vulnerable to infection by external pathogens when "colonization resistance" maintained by healthy gut microbiota is damaged. First, we describe a defense strategy against enteric pathogens using intestinal symbionts. (Chapter 1)

Vibrio cholerae is a causative strain of cholera that leads to dehydration accompanied by acute diarrhea. However, *V. cholerae* infects humans but not mice. The lack of well-

established mouse models has been a major hindrance in cholera research. Therefore, we first attempted to establish a *V. cholerae* mouse model. It was confirmed that treatment with an antibiotic called clindamycin (CL) makes the intestine more susceptible to cholera infection with changes in the intestinal microflora. CL is an antibiotic that selectively kills anaerobic strains of several bacteria. Intestinal microorganisms are composed of several anaerobic bacteria. When CL is administered, many microbes present in the intestine disappear. When mice were treated with CL, it was confirmed that the most remarkably decreased microorganisms were members of the Bacteroides family. The number of microorganisms belonging to Proteobacteria increased. Infection was confirmed after the mice were infected with *V. cholera*e. Thus, we established a mouse model of *V. cholerae* infection using CL. Here, we hypothesized that *V. cholerae* infection was caused by the altered gut microbiota. We believed that *V. cholerae* infection would occur in the gut microbes treated with CL. Therefore, CL-treated feces from mice were transplanted into germ-free (GF) mice to confirm infection with *V. cholerae*. Infection with *V. cholerae* was verified only in GF mice transplanted with CL-treated feces. This showed that the infection of *V. cholerae* was caused by changes in the intestinal microbiota. Here, we confirmed whether the infection of *V. cholerae* was caused by any of the altered intestinal microbes. It was hypothesized that *Bacteroides vulgatus*, which showed the highest change when treated with CL, might be associated with infection with *V. cholerae.* Considering that *V. cholerae* infection occurred in an environment where *B. vulgatus* disappeared, it was supposed that a correlation between *B. vulgatus* and *V. cholerae* existed. The correlation between the two bacteria was confirmed in GF mice. As a result, we showed that the infection of *V. cholerae* was inhibited when *B. vulgatus* was present. Thus, we confirmed that the distribution of intestinal microbes changed when CL was applied. The greatest change was found in *B. vulgatus*, which is predominantly present in the gut microbes of

mice. Infection with *V. cholerae* was confirmed when changes in intestinal microflora were induced. We investigated how the altered gut microbiota was involved in the development of *V. cholerae* infection. It was believed that *V. cholerae* infection was regulated by any environment created by the changed intestinal microbes. Therefore, we tried to identify the environment. The intestinal environment is changed by specific metabolites present in the intestinal microbes. Infection is thought to occur because of this with a focus on metabolites. We found that the metabolites of the intestinal environment induced by changes in the intestinal microbial flora changed the conditions for the proliferation and colonization of *V. cholerae,* making the intestine vulnerable to infection.

While Chapter 1 discusses the importance of commensal microbes in intestinal infections, Chapter 2 addresses the importance of commensal microbes in inflammatory bowel disease (IBD). IBD is a condition in which inflammation is chronically induced in the intestine. According to the location of inflammation, IBD is classified into ulcerative colitis (UC) and Crohn's disease (CD), both of which are chronic inflammatory bowel diseases. Fecal transplantation is often used to treat IBD. By transplanting microorganisms that exist in the intestines of healthy people into patients, the intestinal microorganisms in the dysbiosis state become healthy. Although fecal transplantation is an effective treatment, it has many side effects. Various microorganisms present in the gut are known to us, but some microorganisms remain unknown, which may cause side effects. We created a Major Gut Microbes among Korean (MGMK) strain consortium to alleviate these side effects. It was anticipated that side effects could be alleviated if fecal transplantation was performed using well-known strains. The MGMK strains were selected based on the strains that have been extensively studied among Koreans. We transplanted this MGMK strain into GF mice and investigated how each strain competes for colonization. As a result, we confirmed that *Bacteroides thetaiotaomicron*, *Bacteroides uniformis,* and *Ruminococcus faecis* were

present predominantly. It was confirmed that each strain colonized for 33 days. These three strains were predominantly present around 1 day after strain transplantation and were predominant until the end of the experiment. We named these three strains Strong Intestinal Colonizer 3 (SIC3).

SIC3 was used to verify whether these strains could alleviate IBD. Dextran sulfate sodium (DSS) was administered to mice to create a colitis model. It was confirmed that symptoms were alleviated by treatment with SIC3. When the efficacy of SIC3 was confirmed using several indicators, such as the disease-associated index (DAI), it was found that symptoms were significantly reduced in the group administered SIC3. In other words, it could be verified that SIC3, a commensal microbe, played a significant role in treating IBD.

Overall, it was confirmed that enteric infections can be controlled by commensal microorganisms in the relationship between enteric infections and commensal microorganisms, as described in Chapter 1. In Chapter 2, the possibility of symbiotic microorganisms playing a role in the treatment of IBD was also confirmed.

Key words : Gut microbiota, Inflammatory bowel disease, *V. cholerae, B. vulgatus, B. thetaiotaomicron, B. uniformis, R. faecis*

Beneficial effects of commensal microbes against enteric infection and inflammatory bowel disease

Jin Sun You

Department of Medical Science
The Graduate School, Yonsei University

Directed by Professor Sang Sun Yoon

Chapter 1. Commensal-derived Metabolites Govern *Vibrio cholerae* pathogenesis in Host intestine

I. INTRODUCTION

Vibrio cholerae is the causative agent of pandemic diarrheal disease, cholera. While cholera toxin (CT) and toxin-coregulated pilus (TCP) are known to be the major virulence determinants, its pathogenic mechanisms are starting to be understood as consequences of interaction with indigenous microbes, collectively termed gut microbiota [1-4]. A key feature of the gut microbiota is its protective capacity against enteropathogenic infections, termed "colonization resistance" [5-7]. This property can be ascribed to the microbial ecosystem that is formed within the host intestine. This microbial ecosystem is an ever-changing

community of various microbial species regulated by a complex network of microbiota-intrinsic and microbiota-extrinsic factors [8].

Microbiota-intrinsic factors such as interactions between the gut-residing species serve as the primary determinant of community composition. Such interactions include interbacterial niche competition [9] and secretion of antimicrobial substances [10]. For example, *Bacteroides* species that reside in the human gut, such as *Bacteroides fragilis* and *Bacteroides uniformis*, utilise membrane attack complex/perforin toxins BSAP-1 and BSAP-2 for intraspecies antagonism [11]. Microbiota-extrinsic factors include inflammation, diet, and antibiotic treatment. However, the aforementioned microbiota-intrinsic and extrinsic factors do not operate in exclusion of another. For example, compositional shift induced by an external factor may, in turn, modulate the host immune response via production of specific metabolites [8].

Recent studies have demonstrated that antibiotic treatments alter the gut microbiota in humans and other mammals [12-15], and increase the susceptibility of the host to infections by various enteric pathogens such as *Shigella flexneri* [16], *Salmonella enterica* [17], *Clostridium difficile* [18, 19], and vancomycin-resistant *Enterococcus* [20]. The abolishing effect of antibiotic treatment on host resistance to infection is most likely implemented through a multitude of factors, including suppression of specific microbial species, alteration of the metabolomic landscape as a result of the changed microbiome composition, and/or host responses [21-23]. These findings prompted us to investigate the effects of different classes of antibiotics on the gut microbiota and how they relate to host resistance against *V. cholerae* infection.

In this study, we uncover a unique microbiota-extrinsic treatment that induces severe cholera-like symptoms in adult mice, that are otherwise completely resistant. Furthermore, we show that a dramatic shift in metabolome production profile accounts for the

compromised infection resistance in the host. This report highlights the importance of commensal-derived metabolites as a crucial determinant of host susceptibility to enteric infection.

II. MATERIALS AND METHODS

1. Bacterial strains and growth condition

Vibrio cholerae O1 serotype N16961 was used as a model pathogen in all experiments [24]. N16961 was routinely grown in Luria-Bertani (LB) broth (10 g NaCl, 10 g tryptone and 5 g yeast extract per L) or on LB agar plates (15 g agar per L) at 37 °C under aerobic condition. In order to selectively isolate N16961 from feces, small intestine (SI), cecum and colon, we used streptomycin (Duchefa) at a 200 μg/mL concentration. Another selective medium used to isolate *V. cholerae* from intestinal contents was thiosulfate-citrate-bile salt-sucrose (TCBS) medium. For enumeration of intestinal *V. cholerae* loads, mouse intestines were manually extracted from infected animals. Then the SIs, ceca, and colons were then homogenized in PBS (Sigma-Aldrich) and centrifuged at 1,000 rpm for 1 min. The supernatants were serially diluted in PBS, and spotted on an LB agar plate containing streptomycin. *Bacteroides vulgatus* strains were isolated from C57BL/6 mouse intestines using Bacteroides Bile Esculin (KisanBio, Korea) agar plates. Subsequently, *B. vulgatus* strains were cultivated on Gifu Anaerobic Media (GAM) broth (KisanBio, Korea) in an anaerobic chamber maintained with 90% N2, 5% CO2 and 5% H2. All anaerobic culture media were deoxygenated for at least 24 h prior to usage. RAPD analysis was performed using six different *B. vulgatus* colonies recovered independently from two different CL-treated mice, following procedures described elsewhere [1].

2. Mouse husbandry and antibiotic treatment

Experiments were performed using both specific pathogen free (SPF) and germ-free (GF) mice in C57BL/6 genetic background. SPF mice were obtained from Orient Bio (Sungnam, Korea) and GF mice were generated by the Yonsei University College of Medicine GF mouse facility. Mice were provided sterile water and autoclaved food. GF status was confirmed by negative microbial growth in mouse feces. GF mice were bred and housed in flexible-film isolators (Class Biologically Clean Ltd., Madison, WI). When necessary, GF mice were transferred to isocages (Tecniplast Inc., Italy) for experimental grouping. All mouse experiments were conducted according to the guidelines provided by the Department of Animal Resources of Yonsei Biomedical Research Institute. The Committee on the Ethics of Animal Experiments at Yonsei University College of Medicine approved this study (Permit numbers, 2017-0210 and 2018-0250).

For antibiotic treatment presented in Fig. 1, 8- to 9-week-old C57BL/6 female mice were administered streptomycin (1 mg), Vancomycin (250 μg) and clindamycin (1 mg), or PBS by oral gavage once a day for 5 days. The dosage of the antibiotics was chosen to induce dysbiosis but not complete elimination of commensal species of the gut microbiota. Each oral gavage treatment did not exceed 100 μl. For antibiotic treatment shown in Fig. 1.6, mice were treated with a single dose of CL (10 mg).

3. *V. cholerae* infection and GF mouse manipulation

V. cholerae cells grown aerobically overnight at 37 °C were diluted 100-fold to inoculate fresh LB broth medium. The sub-cultured broth was incubated in a shaking incubator at 37 °C for 4 h. Finally, *V. cholerae* cells were centrifuged at 13,000 rpm for 10 min, and the resulting pellet was suspended in sterile PBS to the concentration of 10^{10} CFU per mL. For infection, 8- to 9-week-old mice were orally infected with 50 μl of *V. cholerae* cell suspension containing approximately 5×10^8 CFU of *V. cholerae* cells. The Fluid accumulation ratio was calculated by the equation (intestine weight) / (total body weight - intestine weight). CT level was quantified by CT ELISA [25]. To enumerate *V. cholerae* cells in mouse feces, fecal pellets were physically disrupted to homogeneity, and fecal suspensions were serially diluted for CFU counting. Shortly after euthanasia, SI, cecum and colon samples were manually extracted from each mouse and homogenized in 5 mL of PBS. The sample homogenates were centrifuged at low speed for remnant tissue removal, and the resulting supernatant was used for CFU counting.

FMT was performed to transplant the antibiotic-treated gut microbiota into GF mice. SPF mice were treated either with CL or PBS as per the procedure described above, and fresh feces were collected 24 h post-antibiotic treatment. In each antibiotic-treated and control group, there were three mice, and two fecal pellets were collected from each mouse. The fecal pellets were pooled per group and suspended in 600 μl of PBS. The suspension was quick-centrifuged to remove the debris, and the resulting supernatants were orally administered. Each GF mouse received 50 μl of FMT solution by oral gavage. For *B. vulgatus* mono-association, *B. vulgatus* was first seeded with thawed stock and passaged at least twice and less than 4 times for maximum viability. *B. vulgatus* cells were grown in Gifu Anaerobic Media (GAM) broth under anaerobic conditions. The cultured *B. vulgatus*

cells were resuspended in PBS, and 10^8 CFU cells were delivered orogastrically to GF mice. Infant mouse infection was performed following procedures described previously [26].

4. Competitive index assay

To proceed with the competitive index assay, *lacZ*-negative wild type strain N16961 and *lacZ*-positive *ΔtcpA* were cultured as per the aforementioned *V. cholerae* culture protocol. Sub-cultured wild type and *ΔtcpA* cells were centrifuged at 13,000 rpm for 2 min and then resuspended in PBS. Each strain was mixed at a 1:1 ratio, and 100 μl of the prepared mixture (total 10^9 CFU) was administered to 8- to 9-week-old female C57BL/6 mice (either untreated or CL-treated) by oral gavage. Each mouse was infected with 5×10^8 CFU of each strain.

5. Amplicon sequencing for microbiome profiling

The extraction method for bacterial DNA was performed by using a PowerMax Soil DNA Isolation Kit (MO BIO). Each sequenced sample was prepared according to the Illumina 16S Metagenomic Sequencing Library protocols to amplify the V3 and V4 regions (519F-806R). The DNA quality is measured by PicoGreenand Nanodrop. Input gDNA (10 ng) was PCR amplified. The barcoded fusion primer sequences used for amplifications were as follows: 341F: 5' CCTACGGGNGGCWGCAG 3', 806R: 5' GACTACHVGGGTATCTAATCC 3'. The final purified product was then quantified using qPCR according to the qPCR Quantification Protocol Guide (KAPA Library Quantificatoin kits for Illumina Sequecing platforms) and qualified using a LabChip GX HT DNA High Sensitivity Kit. (PerkinElmer, Massachusetts, USA). Paired-end (2 × 300 bp) sequencing was performed by the Macrogen using the MiSeq™ platform (Illumina, San Diego, USA). For species identification, sequenced reads were aligned using blast and NCBI 16S microbial database (version downloaded 2018.01.14). Taxonomy information was assigned only to OTUs that met both query coverage > 85% and identity percent > 85%. OTUs that did not meet these two criteria were left unassigned. In general, microbial species was identified with ~ 99% identity with a reference sequence.

6. Metabolite extraction

For extracting ionic metabolites, approximately 50 mg of cecal contents was dissolved in MilliQ water containing internal standards (H3304-1002, Human Metabolome Technologies (HMT), Tsuruoka, Yamagata, Japan) at a ratio of 1:9 (w/v). After centrifugation, the supernatant was centrifugally filtered through a Millipore 5000-Da cutoff filter (UltrafreeMC-PLHCC, HMT) to remove macromolecules (9,100 × *g*, 4 °C, 60 min) for subsequent analysis with capillary electrophoresis time-of-flight mass spectrometry (CE-TOFMS).

7. Metabolome analysis

Metabolome analysis was conducted at HMT using the Basic Scan package with CE-TOFMS for ionic metabolites, based on the methods described previously [27, 28]. Briefly, CE-TOFMS analysis was carried out using an Agilent CE capillary electrophoresis system equipped with an Agilent 6210 time-of-flight mass spectrometer, Agilent 1100 isocratic HPLC pump, Agilent G1603A CE-MS adapter kit, and Agilent G1607A CE-ESI-MS sprayer kit (Agilent Technologies, Waldbronn, Germany). The systems were controlled by Agilent G2201AA Chem-Station software version B.03.01 for CE (Agilent Technologies) and connected by a fused silica capillary (50 μm *i.d.* × 80 cm total length) with commercial electrophoresis buffer (H3301-1001 and H3302-1021 for cation and anion analyses, respectively, HMT) as the electrolyte. The spectrometer was scanned from *m/z* 50 to 1000 [27]. Peaks were extracted using the automatic integration software MasterHands (Keio University, Tsuruoka, Yamagata, Japan) to obtain peak information including *m/z*, peak area, and migration time (MT) for CE-TOFMS analysis [29]. Signal peaks corresponding to isotopomers, adduct ions, and other product ions of known metabolites were excluded, and remaining peaks were annotated according to the HMT metabolite database based on their *m/z* values with the MTs determined by TOFMS. Areas of the annotated peaks were then normalized based on internal standard levels and sample amounts to obtain relative levels of each metabolite. Hierarchical cluster analysis (HCA) was performed using the proprietary software supplied by HMT, PeakStat.

8. *V. cholerae* in vitro growth curve experiments

N16961 was grown in M9 media supplemented with 17 metabolites at 20mM each, with the exceptions of *N*-acetylglucosamine (GluNAc), *N*-acetylneuraminic acid (NANA), glucaric acid, gluconolactone, mannosamine, and cholic acid. These metabolites were added at concentrations 4, 1, 4, 10, 1, and 0.2 mM, respectively. N16961 growth was monitored by measuring OD_{600} values spectrophotometrically. To examine growth-inhibiting capabilities of the metabolites, N16961 was grown in M9 plus 0.4% glucose. However, M9 salt without glucose was used to assess the capabilities of the metabolites to promote the growth of *V. cholerae*.

9. Statistical analysis

Data are expressed as mean ± standard error of the mean (SEM). Unpaired Student's *t*-test were used to determine whether differences between groups were significant. A p value < 0.05 was considered to indicate statistical significance. All experiments were repeated for reproducibility.

III. RESULTS

1. Clindamycin-treated adult mice exhibited dramatic gut microbiota compositional changes and became susceptible to *V. cholerae* infection

Colonization of enteric pathogens occurs depending on the composition of indigenous microbes inside the host intestine [5, 30, 31]. In order to observe the effects of gut microbiota compositional changes on host infection resistance under diverse experimental conditions, we treated adult C57BL/6 specific pathogen free (SPF) mice (8 weeks of age) with three different antibiotics that have a distinct mode of bacterial killing; streptomycin (SM), vancomycin (VAN) and clindamycin (CL). SM is a broad-spectrum antibiotic that targets both Gram-positive and Gram-negative bacteria. VAN is an effective antibiotic against Gram-positives [32], while CL is known to selectively kill anaerobes [33, 34]. After daily treatment for 5 days, mouse feces were collected to analyze microbiota composition by 16S rRNA gene sequencing. Five bacterial phyla were found to have characteristic distributions among groups (Fig. 1.1A-D). In the untreated control group, Bacteroidetes was the most abundant phylum and the members of that single phylum occupied approximately 80% of the entire microbiota population (Fig. 1.1A). Upon SM treatment, the Verrucomicrobia phylum emerged, while the Bacteroidetes phylum maintained its predominant occupancy (Fig. 1.1B). VAN treatment resulted in multiplication of bacterial cells belonging to the Verrucomicrobia and Proteobacteria phyla, both of which are Gram-negatives (Fig. 1.1C). As a result of CL treatment, the Bacteroidetes phylum was eradicated, while the Firmicutes phylum remained largely unchanged in number (Fig. 1.1D). This observation is consistent with previous findings that CL is effective in treating infections of *Bacteroides fragilis*, a

major species of the Bacteroidetes phylum [35, 36]. On the other hand, the Proteobacteria phylum underwent explosive expansion during CL treatment, further demonstrating that CL is not effective in inhibiting the growth of facultative anaerobes (Fig. 1.1D).

Subsequently, the mice of each antibiotic group were infected with 5×10^8 CFU of the *V. cholerae* 7th pandemic strain, N16961, to monitor susceptibility to infection and infection-induced microbiota composition changes. In the control and SM-treated groups, microbiota composition did not change much following *V. cholerae* infection (Figs. 1.1E and F). In response to N16961 infection, the relative abundance of the Bacteroidetes phylum increased in the VAN-pretreated group (Fig. 1.1G vs. 1C). In CL-treated mice, the relative abundance of the Firmicutes phylum increased, while that of the Proteobacteria phylum decreased in response to *V. cholerae* infection (Fig. 1.1H). Importantly, among the Proteobacteria phylum detected in Fig. 1H, ~8.81% was found to be derived from *V. cholerae*-specific 16S rRNA gene sequence (Fig. 1.3). This result is worthy of particular attention because *V. cholerae*-specific sequence was not detected in the Proteobacteria populations in other groups (Fig. 1.1F and G).

Our results indicate that *V. cholerae* may actively colonize the adult mouse intestine under conditions created by CL treatment. To gain more insight into the outcomes of *V. cholerae* infection, we investigated whether any anatomical change was induced in the gastrointestinal tract ranging from the small intestine to the rectum. In the first three experimental groups, mouse tissues appeared similar to one another and no major changes were observed following *V. cholerae* infection (Fig. 1.1I, J, and K). In contrast, infection-induced phenotypes were clearly demonstrated in the CL-treated group for the following indications (Fig. 1.1L). First, fluid accumulation was clearly observed in the small intestine (red arrowheads). Second, the size of the cecum was markedly smaller compared to those in other groups (black arrowhead). Third, the colon appeared shorter and more interestingly,

became transparent, while the colons in other groups were filled with feces (dotted line around the colon). Forth, fecal matter discharged from the CL-treated group were highly aqueous (data not shown). Together, these results demonstrate that *V. cholerae* infection induces cholera-like symptoms in adult mice, when their gut microbiota compositions are altered by CL treatment.

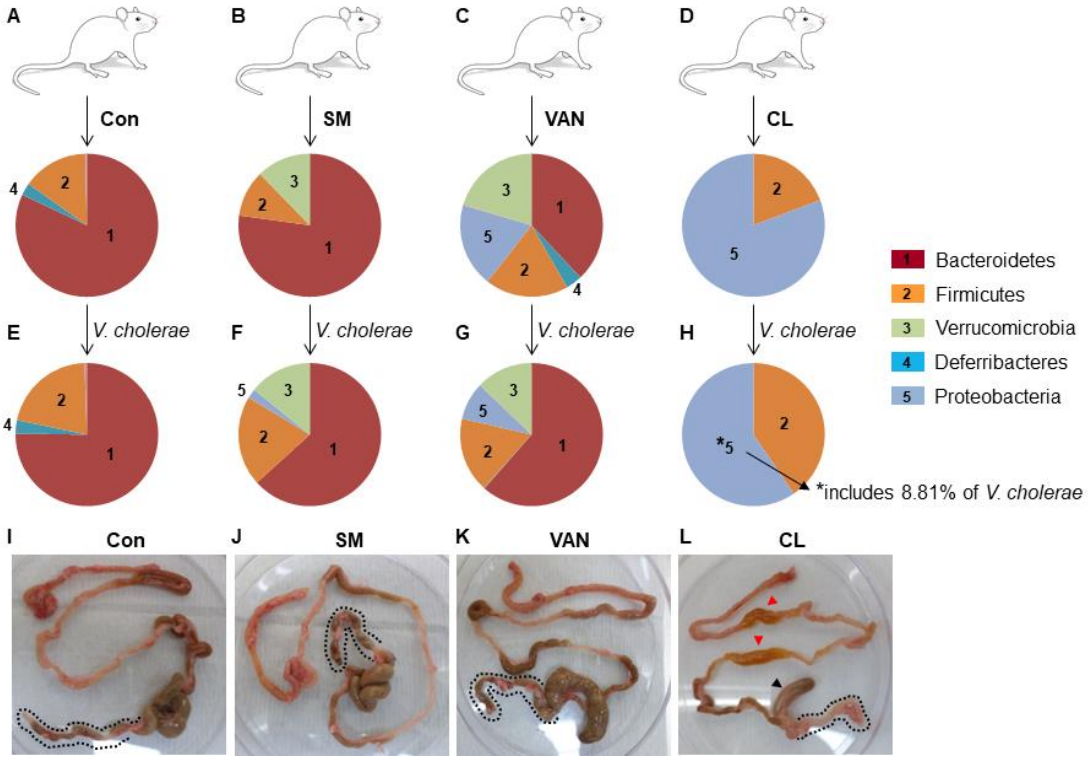

Figure 1.1. Microbial population changes in response to the antibiotic treatments and host responses to *V. cholerae* infection in each treatment group. Adult mice were divided into four groups and treated with PBS (a), streptomycin (SM) (b), vancomycin (VAN) (c), or clindamycin (CL) (d). Treatments were performed as described in "Methods" section. Fecal matter was collected at the end of the treatment, and microbial DNA was extracted for 16S rRNA gene amplicon sequencing. Microbial compositions at the phylum level are shown in pie charts. Relative abundance of each phylum is proportional to the arc length of each slice. Five dominant phyla (i.e., Bacteroidetes, Firmicutes, Verrucomicrobia, Deferribacteres, and Proteobacteria) numbered from 1 to 5 are indicated with different

colors. Following treatment, mice in each group were infected with 5×10^8 CFU of N16961 cells. At 24 h post-infection, fecal matter collected from each group (e–h) was subject to microbial composition analysis. *The Proteobacteria phylum shown in panel H includes *V. cholerae* at 8.81% abundance. At the end of the infection period, mouse gastrointestinal tracks were extracted from each group to visualize infection-induced phenotypes (i–l). Red arrowheads shown in panel l indicate regions of small intestine with fluid accumulation, while a black arrowhead shows the cecum, where the size is remarkably smaller than in other mice. Dotted lines in panels i–l indicate the large intestines.

2. CL treatment with a different regimen similarly induced hypersusceptibility to *V.cholerae* infection

Our results, shown in Fig. 1.1, demonstrate that symptoms of watery diarrhea observed in human cholera patients can also be induced in adult mice by a simple antibiotic pretreatment. In the above experiment, mice were treated with a mild concentration of CL daily for 5 days. To elucidate whether CL treatment could elicit similar effects within a shorter period, we conducted another set of infection experiments with a single treatment of higher CL dosage (Fig. 1.2A). Similar to previous results with lower CL dosage, significantly increased fluid accumulation (FA) was induced in adult mouse intestine at 24 h post-infection. The FA ratio was determined to be ~0.176, a value ~1.6-fold higher in comparison to that of the uninfected group (Fig. 1.2B). Consistent with this finding, robust *V. cholerae* colonization was observed in CL-pretreated mice. The number of *V. cholerae* cells recovered from the small intestine (SI) or cecum was remarkably larger in CL-treated vs. control group. *V. cholerae* cells of $>10^9$ CFU were grown per gram sample in SI and cecum, respectively. Likewise, ~10^9 CFU was also detected in fecal pellets shed from CL-treated mice (Fig. 1.2C). In contrast, *V. cholerae* cells were not detected at all in feces discharged from the control group. Given that an infection dosage of 5×10^8 CFU was used, these results demonstrate that (i) *V. cholerae* cells were almost completely eliminated inside the intestine of regular adult mice while (ii) the same number of inoculated cells was more highly proliferated in the CL-pretreated adult mouse intestine.

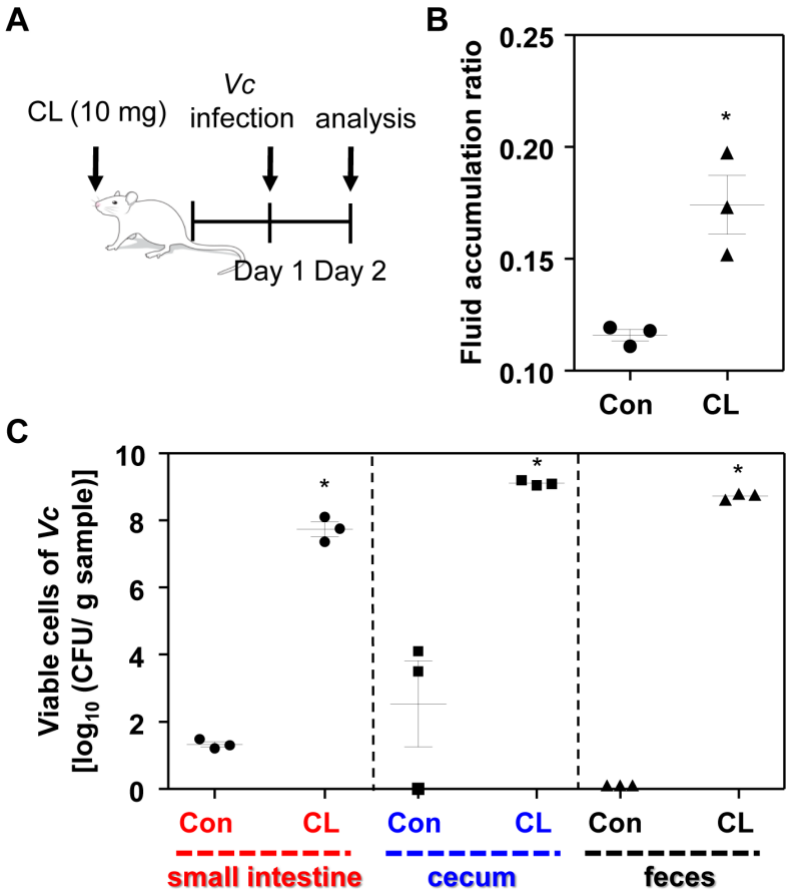

Figure 1.2. Effects of a single-dose treatment of CL on host resistance to *V. cholerae* infection. (A) Schematic diagram of the experimental procedure. C57BL/6 (8~9 weeks old) mice were treated by oral gavage with CL (10 mg/Kg) or PBS as a control. At 24 hr post-treatment, mice were challenged with *V. cholerae* infection (5×10^8 CFU) for 24 hr. (B) At the end of the infection period, fluid accumulation ratio was calculated by the equation of (intestine weight) / (total body weight - intestine weight). *$P < 0.05$ versus the control group. (C) Lysates of small intestine or cecum were prepared by tissue homogenization. Fecal suspensions from each mouse were also prepared by physical grinding. Aliquots of

lysates or suspensions were serially diluted for *V. cholerae* CFU counting on LB agar supplemented with 200 μg/mL SM. Values are expressed as means ± SEM in each treatment group and displayed on a log scale. **P* < 0.001 versus bacterial CFUs detected in the control group.

3. Germ-free mice transplanted with feces of CL-treated mice were susceptible to *V. cholerae* infection

Previous studies have revealed that CL treatment can modulate the production of pro-inflammatory cytokines, especially in response to lipopolysaccharide [37-39]. Furthermore, CL at sub-lethal concentrations stimulate neutrophil phagocytosis in vitro against *Staphylococcus aureus* [40] and *Bacteroides* spp. [41]. While our results strongly suggest that CL-induced changes in gut microbiota composition are associated with elevated susceptibility to *V. cholerae* infection, these previous reports also indicate that enhanced *V. cholerae* infectivity in adult mice might be attributed to CL-induced modulation of the host immune response. To address this issue, we conducted fecal microbiota transplantation (FMT) to germ-free (GF) mice and tested whether the GF mice with reconstituted intestinal microbiota develop differential resistance to *V. cholerae* infection. Fecal pellets freshly collected from PBS- or CL-treated mice were resuspended in PBS and transferred to GF mice via oral gavage. Following a 3-day transplant stabilization period, 5×10^8 N16961 cells were infected (Fig. 1.3A). GF mice transplanted with PBS-treated control fecal pellets developed strong resistance to the infection. Viable *V. cholerae* was recovered neither from the SI of all six mice nor from the cecum isolated from five out of six mice (Fig. 1.3B). While varying degrees of N16961 cells were detected in feces discharged from the GF mice transplanted with control feces, four out of six mice produced feces that contained ten or fewer N16961 cells per gram (Fig. 1.3B). In contrast, N16961 colonization occurred more actively in the GF mice transplanted with CL-treated and therefore Bacteroidetes-depleted feces. In cecum and feces, $>10^4$-fold and $>10^{3.4}$-fold higher bacterial colonization were observed, respectively, compared with the control group (Fig. 1.3B).

We next asked whether production of CT, a critical virulence determinant, was accordingly increased during active *V. cholerae* colonization. As shown in Fig. 1.3C, in response to *V. cholerae* infection, CT production was significantly increased in mice transplanted with fecal suspensions of CL-treated mice. Since CL would not be much left in the feces discharged from the CL-treated mice, our results demonstrate that altered gut microbiota composition induced by CL treatment is directly responsible for rendering the murine host more susceptible to *V. cholerae* infection.

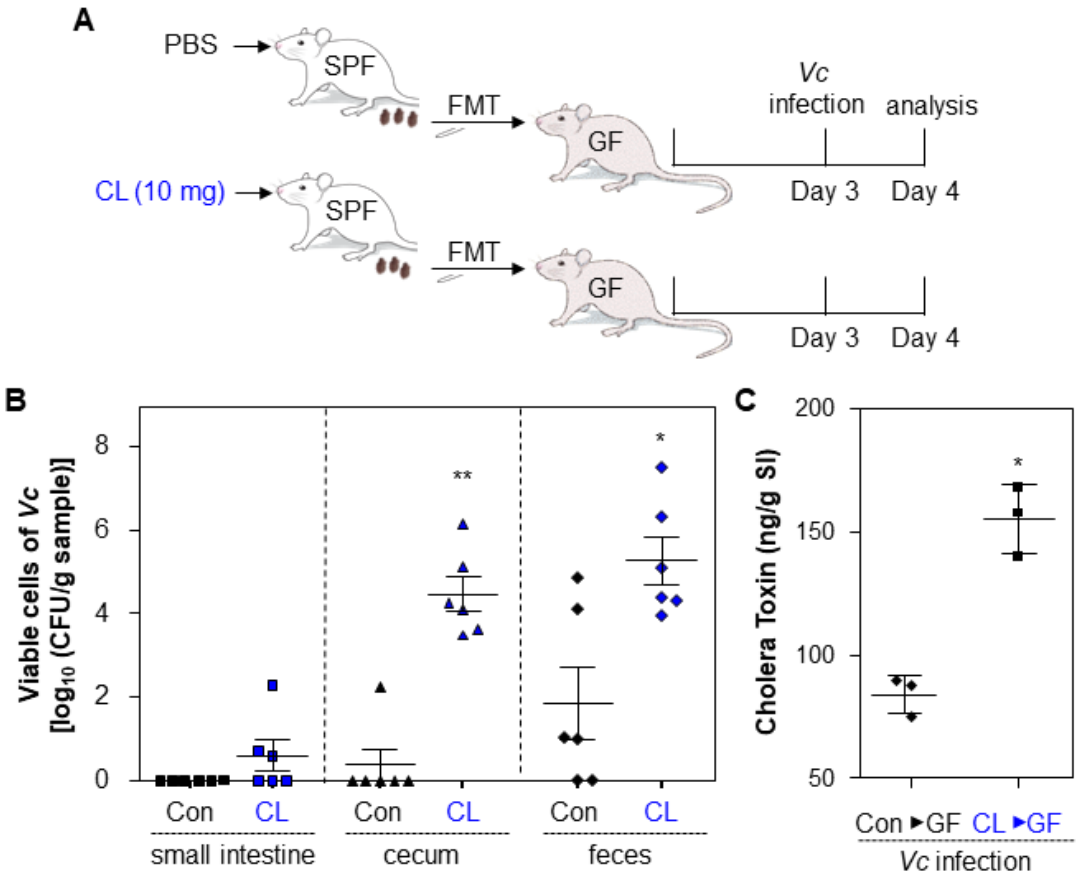

Figure 1.3. Germ-free mice transplanted with feces of CL-treated mice are susceptible to *V. cholerae* infection. (a) Schematic diagram of the experimental procedure. Germ-free mice (C57BL/6, 8~9 weeks old, n = 6 per group) received fecal suspensions (50 μl) derived from PBS- or CL treated SPF mice. Following 3 days of stabilization, transplanted mice were challenged with *V. cholerae* infection (5×10^8 CFU) for 24 h. (b) The SI and cecum were removed from each mouse for tissue homogenization. Fresh fecal matter was collected to prepare fecal suspensions. Aliquots of lysates or suspensions were serially

diluted to count CFU of *V. cholerae* on LB agar supplemented with 200 μg/mL SM. Values are displayed on a log scale as mean ± SEM for each group. **P* < 0.05 versus bacterial CFU detected in the control group. ***P* < 0.001 versus bacterial CFUs detected in the control group. (c) In a separate set of experiments (n = 3 per group), small intestines were extracted for tissue homogenization, and aliquots of homogenates were assessed for detection of CT by ELISA. **P* < 0.01 versus CT level in the control group.

4. *Bacteroides vulgatus* is the predominant species in the Bacteroidetes phylum and it inhibited *V. cholerae* growth in vivo

Based on our results presented in Fig. 1.1, elevated *V. cholerae* infection in CL-pretreated mice could be ascribed either to the depletion of the Bacteroidetes or to the expansion of Proteobacteria phylum. Meanwhile, we noticed the followings. First, the Proteobacteria population similarly sufficiently propagated in VAN-treated mice, a group that did not develop cholera-like symptoms (Fig. 1.1C). Second, the relative abundance of the Bacteroidetes phylum increased from ~38 % (before infection) to ~61 % (after infection) in VAN-treated mice (Fig. 1.1C and G). Based on these results, we postulated that the lack of cholera-like symptoms in the VAN-treated group was due not only to the presence of the Bacteroidetes phylum, but also to the infection-induced expansion of its population. We hypothesized that the Bacteroidetes phylum, which predominantly occupies the adult mouse intestine, plays a critical role in protecting its host from *V. cholerae* infection.

To provide an insight into which bacterial species are core members of the Bacteroidetes phylum, we performed a species-level population analysis using 16S rRNA gene sequencing. When necessary, we conducted PCR reactions with species-specific primer sets and verified the sequences of amplification products (data not shown). Three distinct bacterial species were determined to belong to the Bacteroidetes phylum; *Bacteroides vulgatus, Parabacteroides goldsteinii,* and *Bacteroides caccae*. In control mice, *B. vulgatus* was found to be present in the largest quantity, with a relative abundance greater than 50% of the entire population (Fig. 1.4). In response to VAN treatment, *P. goldsteinii* propagated, whereas *B. vulgatus* was diminished in population size. Of note, however, the relative abundance of the *B. vulgatus* population was recovered to its original level following *V. cholerae* infection. *P. goldsteinii* has been reclassified from *Bacteroides goldsteinii*[42] and

a strain isolated from human intestine was resistant to VAN treatment[43]. As shown in Fig. 1.1D and L, no 16S rRNA gene sequences matching any of these three species were detected in feces discharged from CL-treated mice either before or after *V. cholerae* infection (Fig. 1.4).

Because *B. vulgatus* was the most dominant species in the adult mouse intestine, we next assessed, under a more defined condition, the effect of *B. vulgatus* on altering host susceptibility to *V. cholerae* infection. To this end, we mono-associated GF mice with a suspension of *B. vulgatus* cells, grown anaerobically in vitro (Fig. 1.5A). *B. vulgatus* colonies cultivated straight from mouse fecal suspensions were subject to RAPD assay and an identical amplification pattern was observed between isolated colonies, thereby leading us to conclude that most colonies were clonal (Fig. 1.6). As shown in Fig. 1.5A, GF mice were also mono-associated with heat-killed *B. vulgatus* before being infected with *V. cholerae* cells as an additional negative control. At 24 h post-infection, significantly reduced numbers of *V. cholerae* cells were recovered in animals that were mono-associated with live *B. vulgatus*. In SI and colon, ~830-fold and ~40-fold less *V. cholerae* colonization were observed, respectively, as compared with the PBS control group. Likewise, *V. cholerae* cell numbers, recovered from feces of the GF mice transplanted with live *B. vulgatus*, was ~75-fold lower than the PBS control (Fig. 1.5B). Importantly, *V. cholerae* colonization was never decreased in the animals mono-associated with heat-inactivated *B. vulgatus* cells (Fig. 1.5B). These results suggest that active *B. vulgatus* cells, when present in adult mouse intestine, can suppress *V. cholerae* colonization.

We next explored whether *B. vulgatus* also effectively inhibits *V. cholerae* colonization in the infant mouse model that has been used to study *V. cholerae* infection [25, 26]. Five-day- old infant mice were divided into two groups, with the first group being transplanted with *B. vulgatus* and the other group serving as a negative control (Fig. 1.5C). *B. vulgatus*,

when transplanted in the intestine of the infant mouse, can also effectively suppress *V. cholerae* colonization and fluid accumulation (Fig. 1.5D). *V. cholerae* colonization was decreased ~4.47-fold in the presence of transplanted *B. vulgatus*. Although the difference between these two groups was less pronounced than what was observed in experiments with adult mice, *V. cholerae* colonization and infection-induced fluid accumulation were both reduced significantly in *B. vulgatus*-transplanted infant mice (Fig. 1.5D).

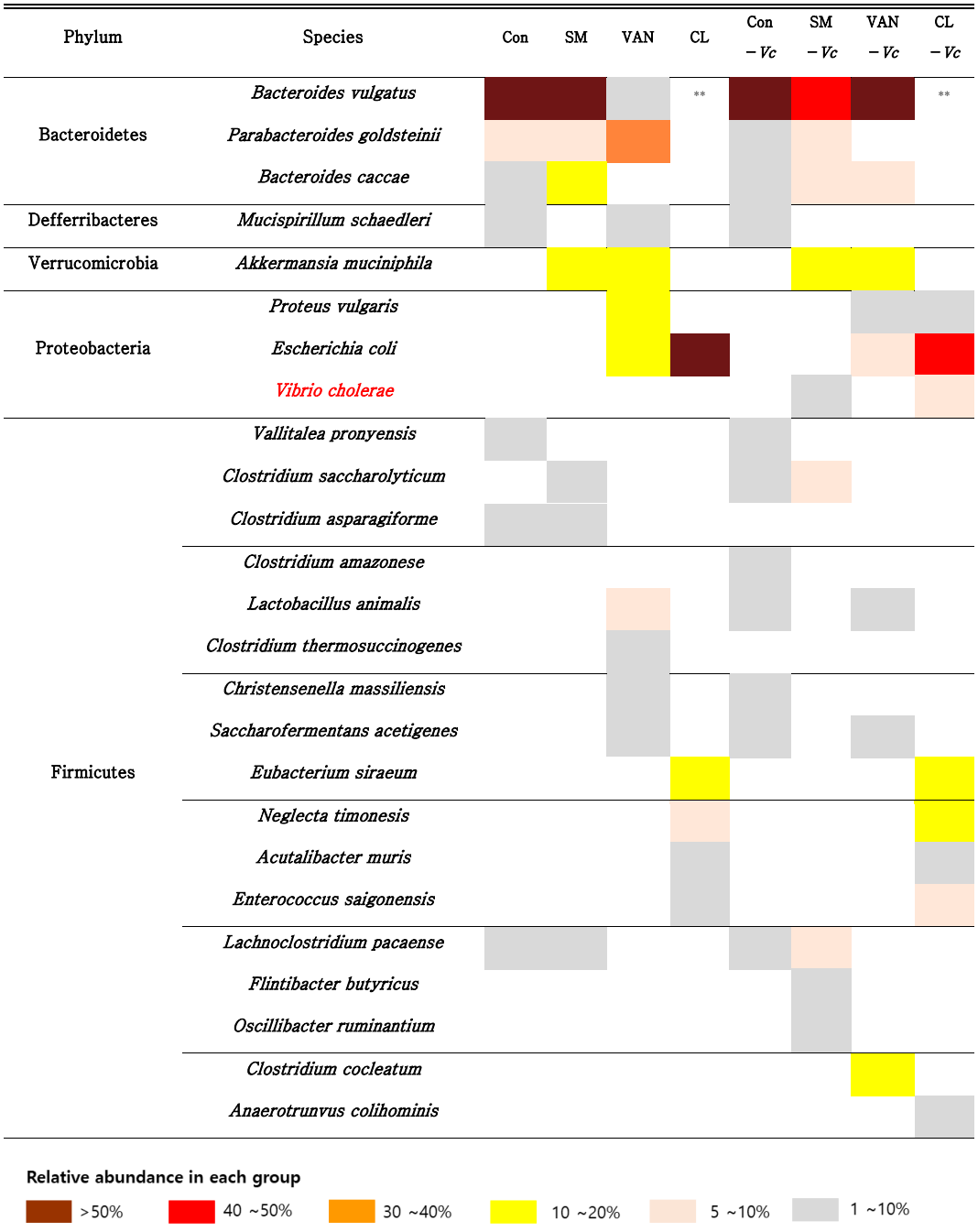

Figure 1.4. Species-level microbiota populations in response to antibiotic treatments and after *V. cholerae* infection. Distribution of commensal microbial species at the phylum (far-left column) and species (second column) levels are presented by colors in 8 different experimental conditions. Con, SM, VAN, and CL in the first low indicate microbial samples of corresponding antibiotic treatments and Con-*Vc*, SM-*Vc*, VAN-*Vc*, and CL-*Vc* indicate samples of the same groups following *V. cholerae* infection. Three species were determined to belong to Bacteroidetes and Proteobacteria phyla and 17 species belonging to the Firmicutes phylum were identified. Only bacterial species with a relative abundance of > % of the total microbiota population were selected and displayed. Relative abundance of each species is indicated by color-coded boxes. For example, brown boxes mean that the abundance of a given species under a specific condition is > 50%. A complete elimination of *Bacteroides vulgatus* is indicated with **, while a pink box denoted by * indicates 8.81% *V. cholerae* occupancy.

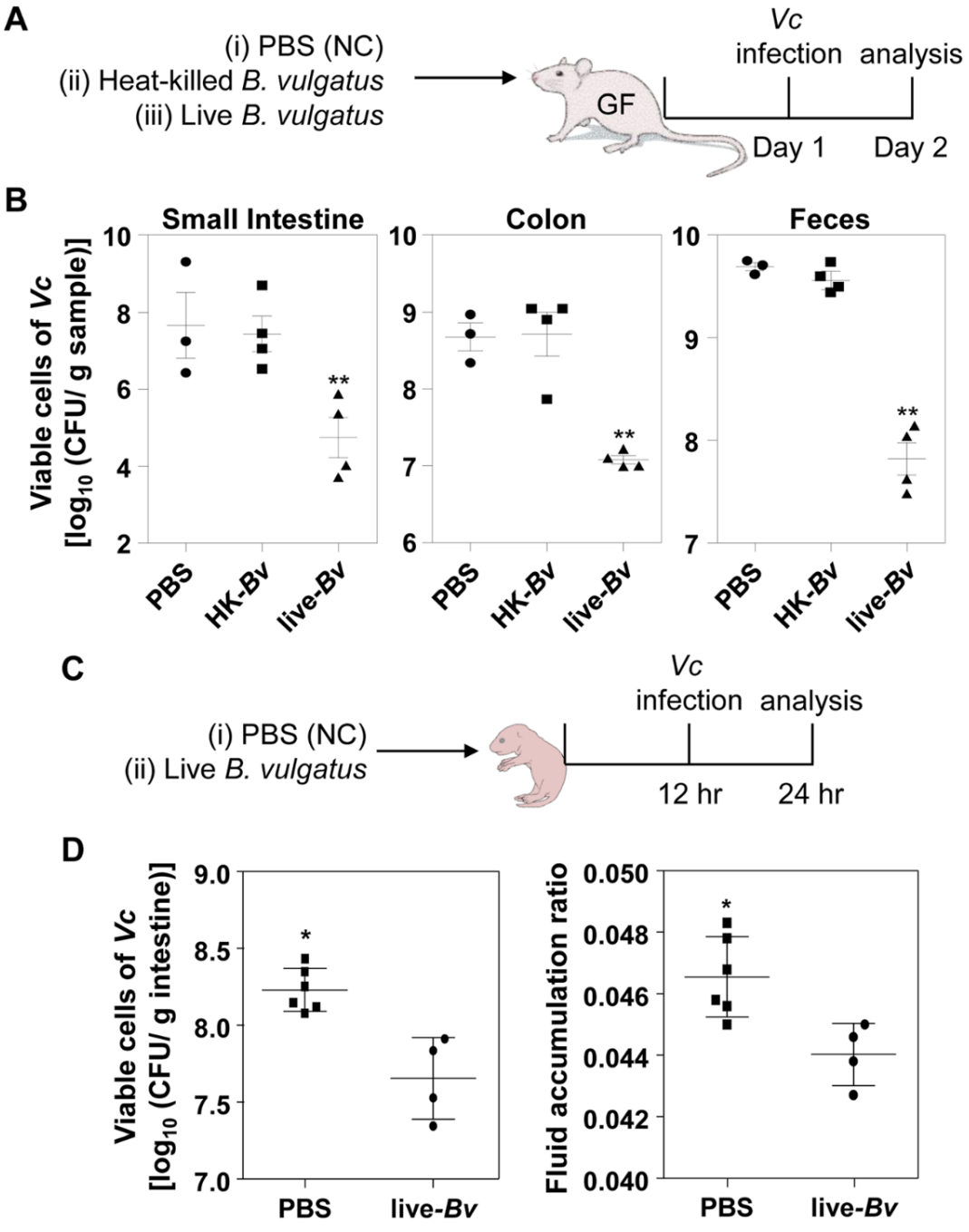

Figure 1.5. *B. vulgatus* inhibits *V. cholerae* growth in vivo. (a) Schematic diagram of the experimental procedure. Germ-free mice (C57BL/6, 8~9 weeks old, n = 3 or 4 per group) ingested 50 μl PBS (n = 3), heat-inactivated (autoclaved) *B. vulgatus* cell suspension (n = 4), or live *B. vulgatus* cell suspension (n = 4). The *B. vulgatus* cell suspensions contained 2×10^9 CFU/mL. At 24 h post-association, mice were challenged with *V. cholerae* infection (5×10^8 CFU) for 24 h. (b) Viable *V. cholerae* cells in SI, colon, or fecal pellets were enumerated and presented in log-scale. $^{**}P < 0.001$ versus bacterial CFU in the control and heat-inactivated *Bv* groups. (c) Schematic diagram of the experimental procedure. Five-day-old infant mice (n = 4 or 6 per group) ingested 50 μl PBS (n = 6) or *B. vulgatus* cell suspension (n = 4). The *B. vulgatus* cell suspensions contained 1×10^9 CFU/mL. At 12 h post-association, mice were challenged with *V. cholerae* infection (1×10^8 CFU) for 12 h. (d) Viable *V. cholerae* cells in intestinal extract were enumerated and presented in log-scale. $^{**}P < 0.05$ versus bacterial CFU in the control group. At the end of the infection period, fluid accumulation ratio was calculated by the equation of (intestine weight) / (total body weight - intestine weight). $^{*}P < 0.05$ versus the control group.

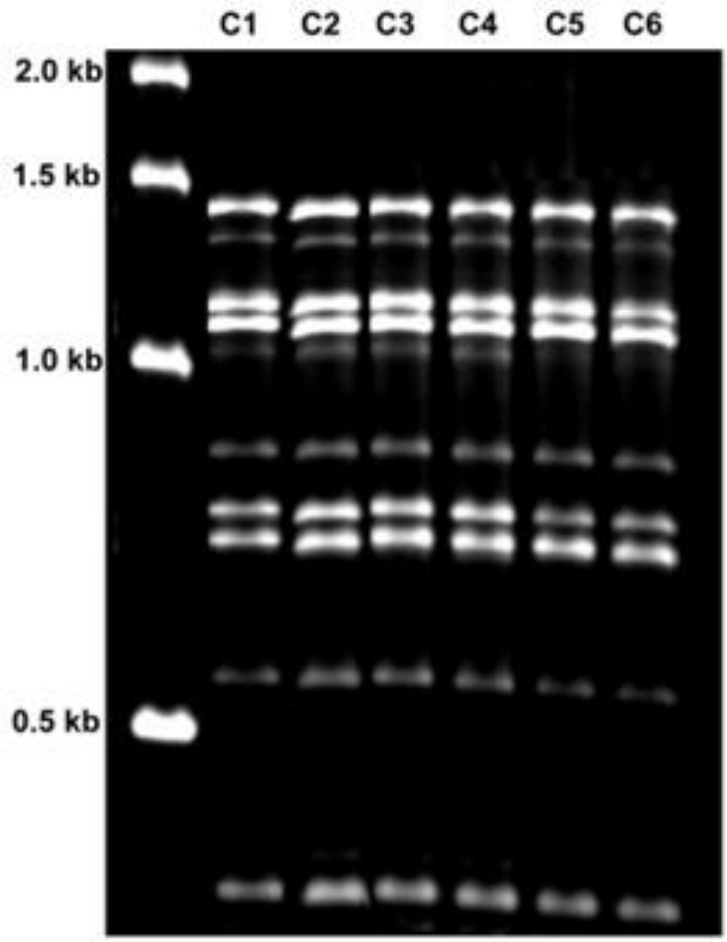

Figure 1.6. Random Amplified Polymorphic DNA (RAPD) analysis of *B. vulgatus* clones. The RAPD amplification reaction was performed as described in "Materials and Methods". Reaction products were analyzed on agarose gels with molecular weight ladders on the far-left lane. A total of 6 colonies isolated from mouse feces were used for the analysis. All of the clones produced identical amplification products.

5. Metabolome profiles revealed the characteristic metabolites that directly modulate intestinal *V. cholerae* growth

We next conducted a metabolome analysis to examine whether metabolomic profiles are altered in response to CL treatment and/or *V. cholerae* infection. We postulated that alterations of metabolite levels influenced host susceptibility to *V. cholerae* infection. Cecal contents were subject to sample preparation for CE-TOF/MS, as described in the "Methods" section. Among the metabolites detected in our analysis, a total of 273 metabolites was successfully quantified and their relative quantities between samples are presented in a heat map (Fig. 1.7). A table that lists all 273 metabolites and their relative amounts in four samples is shown as supplementary information. Of the many differences between the metabolomic profiles of each group, the most noticeable one is that red and green line clusters representing compounds in large and small quantities, respectively, are generally reversed in control SPF vs. CL-treated group (column 1 vs. 3, Fig. 1.7). Such striking alterations in metabolome profiles can be interpreted as a consequence of the dramatic microbiota compositional changes, as shown in Fig. 1. Interestingly, a smaller degree of profile change was observed in response to *V. cholerae* infection in both experimental groups (column 1 vs. 2 and column 3 vs. 4, Fig. 1.7). These results demonstrate that (i) CL treatment induces more substantial changes in metabolome profiles than does *V. cholerae* infection, and (ii) CL-induced changes on metabolite level might have created an environment that strongly facilitates *V. cholerae* growth and pathogenesis.

Table 1 shows a list of metabolites that were detected in the greatest quantities in control SPF (compounds 1~13) or CL-treated (compounds 14~27) mice. Out of the 13 molecules detected in the SPF mouse ceca, all except for cholic acid, were not detected in CL-treated mice. It is of particular interest that (iso)butyric acid, propionic acid, and (iso)valeric acid,

collectively termed short-chain fatty acid (SCFA) are among the most abundantly detected metabolites in control group (Table 1). Fourteen compounds (14~27), whose relative quantities are greater than 1.0E-03, were selected and presented as dominant metabolites in the CL-treated group (Table 1, bottom portion). Relative quantities of those molecules were either non-detectable (compounds 14, 21, 23 and 27) or considerably smaller in the control SPF group. These results further support the notion that distinct profile change occurred in response to CL treatment. We next examined how *V. cholerae* growth is controlled by each of these major compounds. Of the 27 listed compounds, 17 were selected based on the availability and we monitored *V. cholerae* in vitro growth in M9 media supplemented with each metabolite. Growth curve experiments shown in Fig. 1.8 were conducted to reveal compounds that can inhibit *V. cholerae* growth. M9 media used in this particular set of growth experiments contain 0.4% glucose as primary carbon source, thereby enabling us to monitor whether the extraneously added metabolite promotes or inhibits *V. cholerae* growth. Seven metabolites shown in panels K~Q clearly inhibited *V. cholerae* growth. Importantly, these compounds were present in the largest quantities in regular SPF mouse intestines, but either absent or barely detectable in CL-treated mouse intestines (Table 1). Prominent growth promotion was observed when the culture medium included NAG (Fig. 1.8B), a metabolite detected at sufficiently high level in CL-treated mice. Supplementation with urea (Fig. 1.8A), glucaric acid (Fig. 1.8F), putrescine (Fig. 1.8I), or fumaric acid (Fig. 1.8J) resulted in a slight growth stimulation, especially during the early stage of growth. Again, these metabolites were detected more abundantly in CL-treated mice, than in the SPF control mice (Table 1). When N16961 growth was assessed in M9 media with an indicated metabolite as the sole carbon source, each metabolite's ability to stimulate *V. cholerae* growth was clearly demonstrated (Fig. 1.9). Consistent with result shown in Fig. 8B, NAG was most potent in stimulating *V. cholerae* growth, with

OD_{600} values reaching ~1.05 (Fig. 1.9B). Next to NAG, gluconic acid (Fig. 1.9D) and gluconolactone (Fig. 1.9G) were effective at promoting *V. cholerae* growth. As expected, seven inhibitory metabolites (cholic acid, butyric acid, isobutyric acid, propionic acid, valeric acid, isovaleric acid and trimethylamine) still prevented growth of *V.cholerae* (Fig. 1.9K~Q). Together, these results illustrate that CL-induced changes in the host intestine are clearly reflected on metabolite level and such major alterations of metabolomic profiles significantly affect *V. cholerae* intestinal growth.

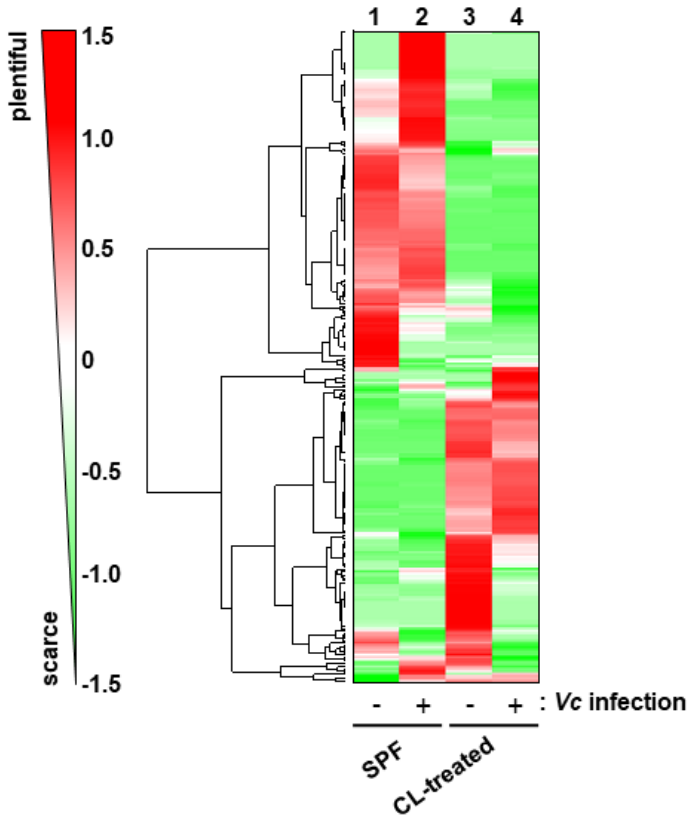

Figure 1.7. Heat map constructed from hierarchical cluster analysis (HCA) of cecal metabolites. Metabolites (n = 273) that exhibit similar detection patterns in four samples are clustered, and the distance between clusters is shown as a tree diagram. The degree of red or green color indicates a larger or smaller amount of a given metabolite. Columns 1 and 2 display metabolome profiles of regular SPF mice, while 3 and 4 shows those of CL-treated groups. Columns 2 and 4 are metabolome profiles after *V. cholerae* infection in each group.

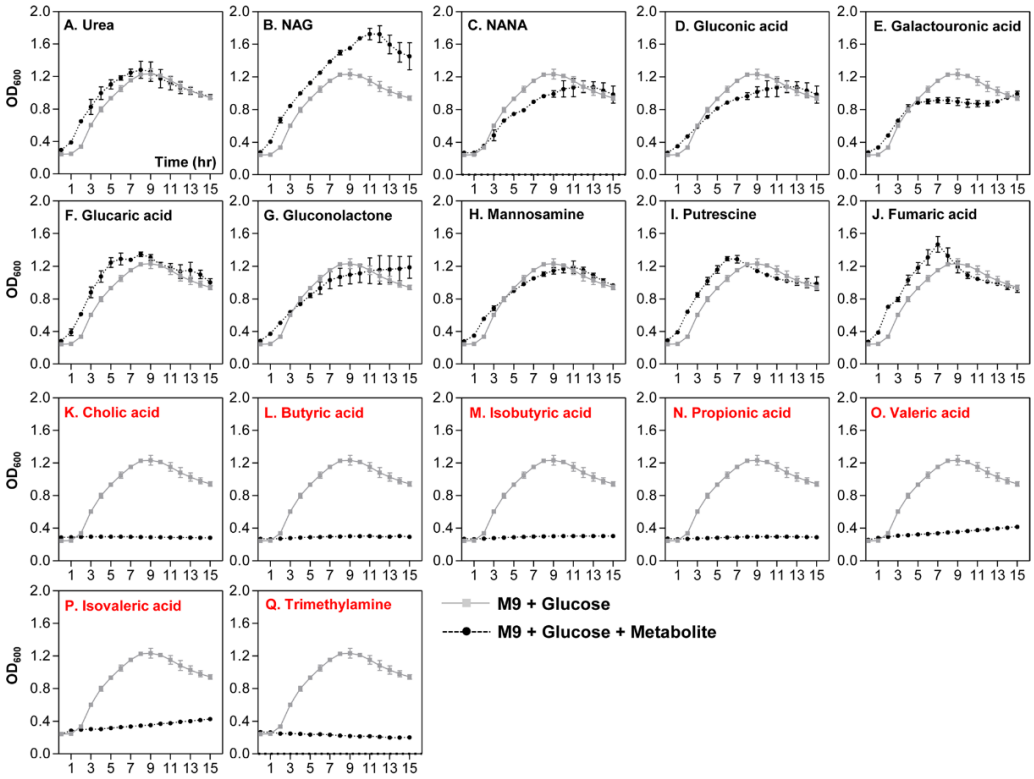

Figure 1.8. Effects of selected metabolites on the inhibition of *V. cholerae* growth in vitro. N16961, a 7th pandemic *V. cholerae* strain, was grown in the presence of indicated metabolites in M9 media. A total of 17 metabolites were tested. Medium pH was neutralized by adding NaOH or HCl, when necessary. OD_{600} values were measured to monitor bacterial growth every 2 h. M9 media contains 0.4% glucose as a primary carbon source. Lines in gray show bacterial growth in M9+glucose (M9G), while black lines indicate bacterial growth in M9G supplemented with indicated metabolites. Cholic acid (panel K), Butyric acid (panel L), Isobutyric acid (panel M), Propionic acid (panel N), Valeric acid (panel O), Isovaleric acid (panel P), and Trimethylamine (panel Q) are highly capable of inhibiting N16961 growth.

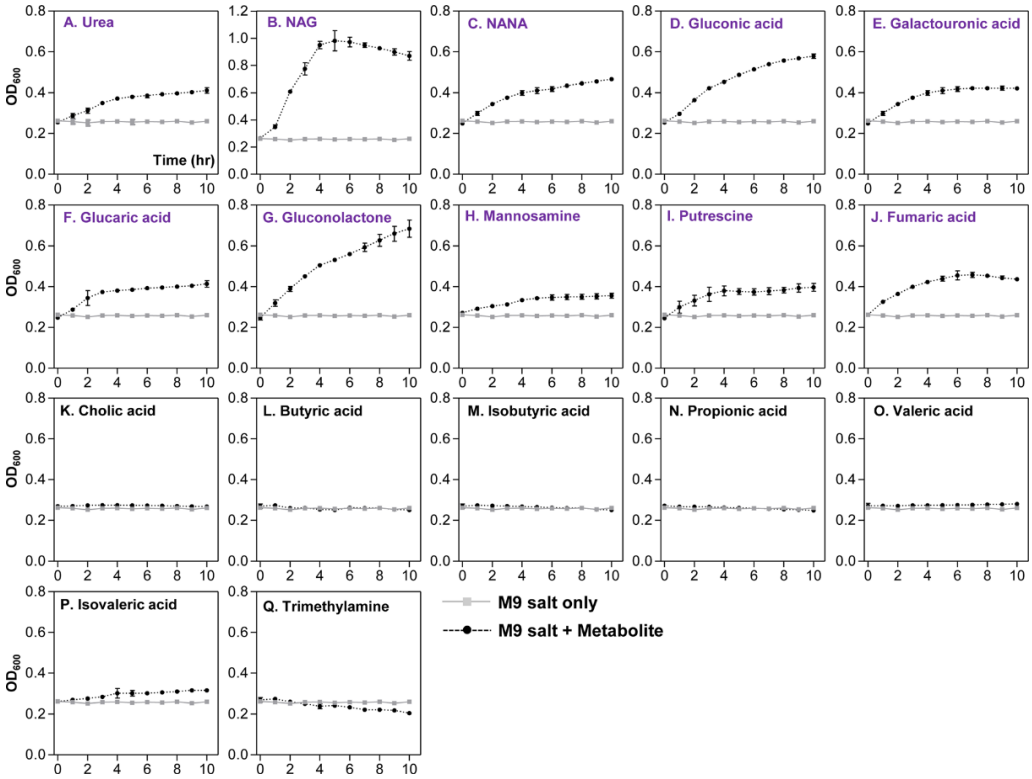

Figure 1.9. Effects of selected metabolites on the stimulation of *V. cholerae* growth in vitro. Bacterial growth was conducted as described in Fig. 1.8. To examine growth-stimulating capabilities of metabolites, M9 media lacking in glucose was used in experiments. Lines in gray show bacterial growth in M9 with no carbon source, while black lines indicate bacterial growth in M9 supplemented with indicated metabolites. Compounds shown in purple font promoted bacterial growth, albeit to varying degrees. The degree of growth-promoting capability of a given metabolite is displayed semi-qualitatively with "+++", "++", or "+" in Table 1. "+++" indicates the metabolite with the strongest growth-promoting capability, while the "+" means that the metabolite induced a mild growth promotion.

		Metabolites	m/z	MT/RT	Relative quantity				*Vc* growth
					SPF	SPF-Vc	CL	CL-Vc	
Dominant in SPF control mice	1	Butyric acid / Isobutyric acid	87.046	10.12	2.1E-01	2.6E-01	ND	ND	--- / ---
	2	Cholic acid	407.282	6.94	6.8E-02	1.4E-02	2.3E-04	ND	---
	3	Propionic acid	73.031	11.11	4.8E-02	3.9E-02	ND	ND	---
	4	Valeric acid / Isovaleric acid	101.062	9.46	2.0E-02	1.4E-02	ND	ND	--- /---
	5	Trimethylamine	60.081	5.78	1.9E-02	3.8E-02	ND	ND	---
	6	Glucose 6-phosphate	259.024	10.12	1.8E-02	5.3E-02	ND	ND	NT
	7	Fructose 6-phosphate	259.023	10.15	3.7E-03	1.0E-02	ND	ND	NT
	8	2-Hydroxyglutaric acid	147.031	17.02	2.9E-03	3.7E-03	ND	ND	NT
	9	2-Oxoglutaric acid	145.014	21.85	2.8E-03	2.3E-03	ND	ND	NT
	10	*N*-Acetylglutamic acid	188.057	13.44	2.7E-03	1.7E-03	ND	ND	NT
	11	3-(4-Hydroxyphenyl) propionic acid	165.056	8.49	2.4E-03	4.7E-03	ND	ND	NT
	12	*trans*-Glutaconic acid	131.035	25.78	2.2E-03	2.2E-03	ND	ND	NT
	13	*N*-Acetylaspartic acid	174.042	14.88	2.2E-03	8.8E-04	ND	ND	NT
Dominant in CL-treated mice	14	Urea	61.040	23.47	ND	ND	1.7E-01	2.8E-01	+
	15	*N*-Acetylgalactosamine / *N*-Acetylmannosamine / *N*-Acetylglucosamine	222.098	24.67	7.2E-03	3.3E-03	5.6E-02	1.0E-02	NT / NT / +++
	16	*N*-Acetylneuraminic acid	308.100	7.33	1.2E-03	4.0E-04	5.2E-02	4.3E-02	+
	17	Creatinine	114.067	7.27	6.5E-04	1.2E-02	3.1E-02	5.0E-02	NT
	18	Gluconic acid	195.051	8.28	9.2E-04	1.7E-03	1.6E-02	1.8E-02	++
	19	Gulonic acid	195.051	8.21	4.3E-04	ND	1.6E-02	2.8E-03	NT
	20	Glucuronic acid-1 / Galacturonic acid-1	193.036	8.36	4.5E-04	3.0E-04	1.2E-02	2.0E-03	NT / +
	21	Glucaric acid	209.031	14.81	ND	ND	1.0E-02	1.3E-02	+
	22	Gluconolactone	179.055	25.71	9.5E-04	9.1E-04	8.2E-03	1.1E-02	++
	23	Galactosamine Glucosamine	180.086	9.36	ND	3.9E-04	2.1E-03	6.8E-04	NT
	24	Mannosamine	180.088	9.07	4.2E-04	6.8E-04	2.0E-03	2.6E-03	+
	25	Putrescine	89.108	4.60	2.4E-04	3.1E-04	1.6E-03	4.6E-03	+
	26	*N*-Acetylalanine	130.051	9.03	1.5E-04	1.1E-04	1.2E-03	1.2E-03	NT
	27	Fumaric acid	115.004	26.01	ND	ND	1.1E-03	8.2E-04	+

Table 1. Metabolites found to be dominant in regular SPF and CL-treated mouse intestines and their impacts on *V. cholerae* growth. Twenty-seven metabolites that were present exclusively in either group were selected among 273 compounds. Metabolites detected most abundantly in the control group (No.1~13) or in the CL-treated group (No.14~27) are listed in the order of quantity. The growth-inhibiting or growth-promoting capability of a given metabolite is displayed semi-qualitatively with a minus (-) or plus (+)

sign, respectively. For example, “+” indicates a metabolite with mild growth-promoting capability, whereas “---” indicates that the metabolite induced strong growth suppression. *ND* not detected, *NT* not tested, *m/z* mass-to-charge ratio, *MT* migration time, *RT* retention time, *Vc Vibrio cholerae*. Relative quantity of a metabolite is calculated by the equation: (peak area of the metabolite) / (peak areas of internal standards × sample amount). Peaks are assigned based on the signal-to-noise ratio (S/N) of 3 or above.

6. CL-treated adult mice can serve as a model for investigating *V. cholerae* pathogenesis

Our results demonstrate infection-induced phenotypes, such as intestinal colonization and fluid accumulation, are clearly observed in CL-pretreated adult mice. Therefore, we finally examined whether or not CL-treated mice can be utilized as a model to delineate *V. cholerae* infection. To address this issue, two groups of mice were infected with 1:1 mixture of N16961 and its *ΔtcpA* mutant, a well-characterized *V. cholerae* mutant defective in colonizing the intestine[44]. We then compared colonization capabilities of these two strains by calculating the competitive index. In this particular set of experiments, fluid accumulation and bacterial colonization were again substantially increased in CL-treated mice, but not in PBS-treated control group (Fig. 1.10). *V. cholerae* cells were completely eliminated in three out of six mice in control group (Fig. 1.11A). Importantly, *ΔtcpA* mutant exhibited significantly reduced colonization capabilities, in comparison to WT N16961 (Fig. 1.11B). The average values of the competitive indices (*ΔtcpA* / WT) were ~0.29 and ~0.28 in the small intestine and cecum of CL-treated mice, respectively. In contrast, meaningful differences in colonization capabilities between two strains were not detected, when untreated adult mice were used (Fig. 1.11B). These results suggest that CL pretreatment not only induces active bacterial colonization, but also creates a valuable environment we can exploit to better understand the pathogenesis of *V. cholerae*.

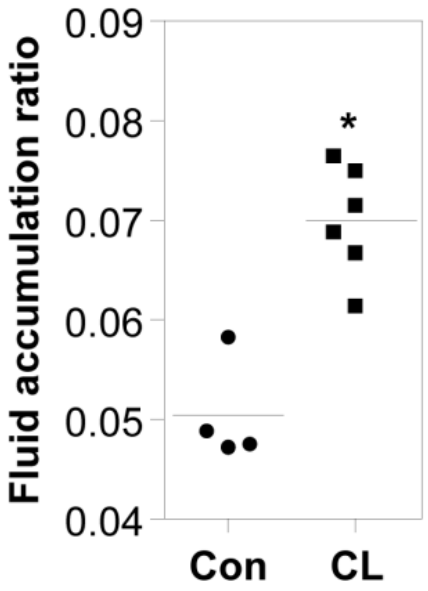

Figure 1.10. A *V. cholerae ΔtcpA* mutant is defective in colonizing the intestine of CL-treated adult mouse. N16961 and its *ΔtcpA* mutant grown in LB were harvested and mixed at 1:1 ratio. A mixture of 2×10^8 CFU was inoculated via oral gavage into PBS-treated (control, n=4) or CL-treated mice (n=6). At 24 h post-infection, mice were sacrificed to measure fluid accumulation ratio. *$P < 0.05$ versus the control group.

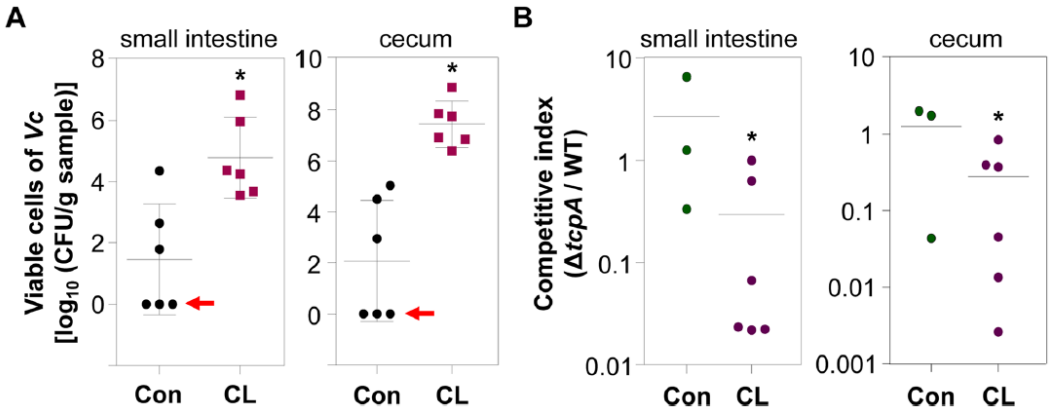

Figure 1.11. A *V. cholerae ΔtcpA* mutant is defective in colonizing the intestine of CL-treated adult mice. N16961 and its *ΔtcpA* mutant grown in LB were harvested and mixed at 1:1 ratio. A mixture of 1×10^9 CFU was inoculated via oral gavage into PBS-treated (control) or CL-treated mice (n = 6 per group). At 24 h post-infection, mice were sacrificed to measure bacterial colonization. (a) Viable cell numbers of *V. cholerae* cells (both N16961 and the *ΔtcpA* mutant). Aliquots of lysates (small intestine or cecum) were serially diluted for *V. cholerae* CFU counting on LB agar supplemented with 200 μg/mL SM. Values are displayed on a log scale as mean ± SEM for each group. **P* < 0.05 versus bacterial CFUs detected in the control group. In three out of six mice in the control group, no *V. cholerae* cells were recovered in the small intestine or cecum (red arrows). (b) The competitive index represents the ratio of *ΔtcpA* mutant to N16961 recovered after infection either in the small intestine or cecum in each mouse after infection. **P* < 0.05 versus the competitive index obtained from infection with no CL treatment.

IV. DISCUSSION

A long-standing unresolved question in cholera research is how *V. cholerae* has evolved as a human-specific pathogen in nature. It has been of particular interest that GM1 ganglioside, a lipid molecule that binds to CT, is present not only on human intestinal epithelium but also mouse intestinal epithelium [45, 46]. This notion suggests that CT, the most important virulence determinant in *V. cholerae*, should also be active in mouse intestine. However, adult mice are naturally resistant to *V. cholerae* infection. We hypothesized that understanding compositional differences between human and mouse intestinal microbiotas would help address this important issue of host tropism.

Our 16S rRNA gene sequencing data (Figs. 1.1 and 1.4) show that approximately 80% of the C57BL/6 mouse gut microbiota belongs to the Bacteroidetes phylum. Virtually complete elimination of the phylum induced by CL treatment is essential for infecting the murine host with *V. cholerae.* However, for our findings to be clinically relevant, it needs to be first established that the mouse gut microbiome is, to a sufficient degree, reflective of the human gut microbiome. Previous studies have reported predominantly high relative abundances of the *Bacteroidetes* phylum in both mouse and human gut microbiomes [47-50]. Furthermore, there is evidence that *B. vulgatus* isolates from human and other animal hosts are indistinguishable based on their 16S rRNA gene sequences [51], suggesting phylogenetic proximity between mouse- and human-gut resident *B. vulgatus* strains. Nonetheless, the composition of a gut microbiome does not necessarily reflect its functional capacity [50]. Additionally, even though the mouse gut microbiome closely resembles that of humans at the phylum level, the similarity dissipates on lower taxonomic levels, as families and genera that comprise the predominant *Bacteroidetes* phylum are quite different between

mice and humans [48]. To compensate for such limitations, we have demonstrated that our key findings are reproduced when GF mice are mono-associated with *B. vulgatus* and infected with *V. cholerae* (Figs. 1.5A and B). Given such considerations, it is likely that the relative abundance of *B. vulgatus* is an important determining factor for *V. cholerae* infectivity not only in murine hosts but in humans as well. An important question would be how abundantly *B. vulgatus* cells that share similar functions with mouse isolates are present in human intestine.

Based on our species-level population changes, *Escherichia coli* explosively proliferated during CL treatment and became the most dominant component (Fig. 1.4). This finding suggests that elevated susceptibility to *V. cholerae* infection in CL-pretreated mouse could also be due to the presence of *E. coli* cells in large quantity. In line with this notion, an *E. coli* strain with robust catalase activity was found to stimulate enhanced *V. cholerae* intestinal colonization in neonatal mice [1]. In the same work, increased *V. cholerae* colonization occurred in VAN-treated adult mice [1]. In the current study, however, cholera-like symptoms including fluid accumulation in the small intestine and production of watery fecal matter were not observed in the VAN-treated group (Fig. 1.1K). We therefore conclude that the loss of *B. vulgatus* is a much more critical determinant over increased *E. coli* for host susceptibility to *V. cholerae* infection.

In the present study, we found that CL treatment increases *V. cholerae* infectivity in the normally resistant adult mice. Previous studies have reported that antibiotic administration triggers dysbiosis in the gut microbiota [52, 53], and such perturbations lead to suppression of host resistance against various enteropathogenic infections. Since CL treatment results in significant perturbation of the gut microbiome, it is conceivable that this model would demonstrate increased susceptibility to infections by other enteric pathogens such as *Salmonella enterica* serovar Typhimurium, *Citrobacter rodentium,* and *Clostridium*

difficile. However, for the aforementioned enteric pathogens, there already exists a well-established adult mouse model [54, 55]. Here, we suggest a simple and convenient animal model to study *V. cholerae* infection. The adult mouse model treated with oral CL consistently exhibited cholera-like symptoms. Out of the several already-existing animal models for cholera research, the suckling mouse model is considered to be a descriptive model that manifests the cholera-characteristic watery diarrhea. However, the model is not adequate for use in vaccine research, because suckling mice have yet to develop adaptive immunity[56]. Moreover, the susceptibility of suckling mice to *V. cholerae* infection might be an artifact caused by their immature immune system, although this idea has not yet been fully verified. Therefore, an infection model using adult mouse has been required for the purpose of unveiling the pathophysiological mechanisms that *V. cholerae* employs to induce cholera in the host intestine [57]. However, intestinal fluid secretion and continuous colonization of *V. cholerae* do not readily occur in adult mice harboring intact gut microflora [58, 59]. For this reason, the ligated ileal loop model that involves surgical manipulation of the animal's intestine has been proposed as an alternative [60]. Our CL-induced adult mouse model, which can be established by a simple treatment, clearly reproduces typical cholera symptoms observed in humans, such as the severe watery diarrhea, extensive fluid accumulation, and *V. cholerae* colonization within the intestinal mucus layer. Furthermore, in our model, CT has been detected in the intestinal fluid, at a level sufficient to elicit intestinal fluid secretion (Fig. 1.3C). In addition, the competitive index of *ΔtcpA* / WT showed that TCP, a verified colonization factor of *V. cholerae* in human intestine [61, 62], is also essential for the induction of illness in adult mice (Fig. 1.11). To date, the importance of TCP has been explored only in infant rabbits [57] and infant mice [63].

Host-derived mucus glycan is a nutrient source utilized exclusively by the gut microbiota.

Considering the microbial competition for nutritional resources in the intestinal tract and constant release of glycan into the lumen by epithelial cell turnover [64-66], the ability of select microbes to nutritionally exploit the glycans confers a conceivable advantage toward their survival and proliferation. A large proportion of glycan structures consist of *N*-acetyl amino sugars, such as *N*-acetylgalactosamine (GalNAc), *N*-acetylglucosamine (GlcNAc, NAG), and *N*-acetylneuraminic acid (Neu5Ac, NANA). Monosaccharides are produced as the result of mucin glycans being catabolized by the gut microbial species equipped with glycosidase genes. *Bacteroides* has evolved to express glycosidase genes which allow them to perform mucin degradation to full completion, and thus become well-adapted to thrive in the intestine [65-67]. The anaerobes that belong to the Bacteroidetes phylum and *Clostridia*, produce pyruvate through glycolysis [65, 68]. Under the anoxic conditions of the intestine, the gut microbiota obtains additional energy by exploiting the pyruvate through anaerobic catabolism. Predominant end products of the anaerobic fermentation are short-chain fatty acids (SCFAs), such as propionic acid, butyric acid and valeric acid [65].

In this study, the dramatic changes in the cecal metabolomes of CL-treated mice strongly correlate with the compositional shift of the microbiota. Depletion of SCFAs and relatively high occurrence of amino sugars in the ceca of CL-treated mice indicate that catabolism of mucin glycan, a proliferation strategy for microbes belonging to the Bacteroidetes phylum, became inactive upon CL treatment.

Utilization of the host glycan is also important for the invasion of *V. cholerae* into the host intestine. When the pathogen enters the intestinal tract, the next strategy for its proliferation is to colonize the epithelial cells covered with a viscous layer of mucus. *V. cholerae* effectively responds to the mucus glycan and catabolize the polysaccharides to acquire competitive advantage in host intestine [69-72]. Glucosamine-6-phosphate (GlcNP-6), a common intermediate molecule shared between the catabolic pathways of GlcNAc

and Neu5Ac, was reported to be indispensable for *V. cholerae* motility [72]. Chemotaxis mediated by motility toward the nutrient sources is important for colonization and proliferation of *V. cholerae* [72]. Consistent with this notion, depletion of sialic acid (Neu5Ac) transporters (encoded in *VC1777-1779*) attenuates colonization [73]. During this process, *V. cholerae* needs to overcome a number of challenges such as acid stress, antimicrobial peptides, host immune response, and SCFAs [68, 70, 72]. The reduction of intestinal SCFAs in patients with diarrhea and recovery of normal SCFA levels after conventional treatment, support that the SCFAs could be a contributing factor to eubiosis of the intestinal microbiota [74]. In general, SCFAs are considered to be an effective barrier against pathogenic invasion, although some enteric pathogens exploit SCFAs to sense their surroundings and to decide whether or not to express their arsenal of virulence factors [75].

Our results suggest that catabolism of *N*-acetyl amino sugars and subsequent accumulation of SCFAs in the distal intestine are largely managed by specific gut microbiota (Fig. 1.4). Elimination of the anaerobic *Bacteroides* and *Clostridium* genera caused by CL treatment results in drastic changes of intestinal metabolites as summarized in Fig. 1.12. Especially, propionic and butyric acid mainly produced by *Bacteroides* and *Clostridium*, respectively, are dramatically reduced after CL treatment, thus leaving a variety of metabolites (NAG, NANA, gluconate, gluconolactone, etc.) available for utilization by *V. cholerae* (Fig. 1.12). Of particular note, gluconate and its intermediate metabolites were found to enhance the colonization and virulence of *V. cholerae* within the intestine [76]. In the perturbed intestinal environment, *V. cholerae* readily acquires nutrient sources as there is no competition with the host glycan-degrading and thus SCFA-producing gut microbiota (mainly *Bacteroides* and *Clostridium)* genera.

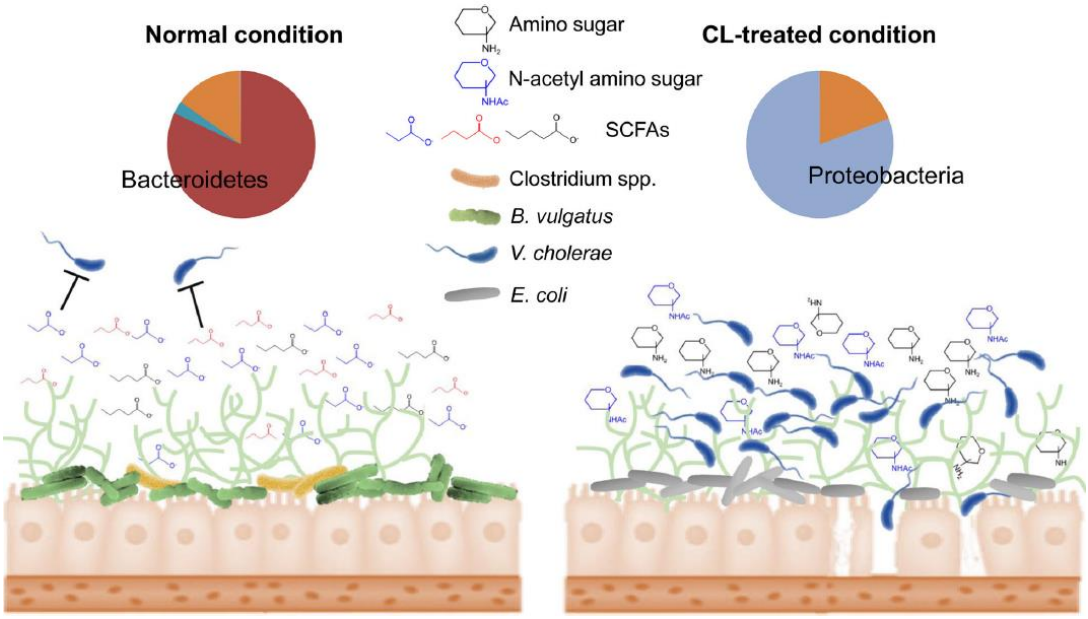

Figure 1.12. Summary of CL-induced microbiota composition changes and its impact on host susceptibility to *V. cholerae* infection. A remarkable shift in commensal microbiota population occurs in response to treatment with CL. Under normal condition, *B. vulgatus*, and to a lesser degree, also Clostridium spp. metabolize mucin glycan and accumulation of metabolites including SCFAs that suppress *V. cholerae* intestinal growth ensues. Metabolites that increased in quantities upon CL treatment, such as amino sugars, potentiate *V. cholerae* intestinal growth.

V. CONCLUSION

In conclusion, we identified a commensal bacterial species, *B. vulgatus*, that plays a significant role in inhibiting *V. cholerae* colonization in the adult mouse intestine. Moreover, we propose a simple antibiotic-treated mouse model to delineate *V. cholerae* infection, which might prove a useful tool for cholera vaccine research. We hope that the results presented in the present study will stimulate future investigations to better understand the in vivo probiotic functions of *B. vulgatus* against *V. cholerae* infection and to devise better strategies for tackling this virulent and clinically important human pathogen.

Chapter 2. A consortium of commensal microbes alleviates diseased symptoms by persistent intestinal colonization

I. INTRODUCTION

The gut microbiome comprises trillions of microorganisms. In most people, the gut microbiota, composed of four phyla, exists in a balanced manner, with Firmicutes and Bacteroidetes being predominant [77-81].

These intestinal microbes affect various functions of the host. Research has suggested that there is a correlation between various diseases and gut microbes [82, 83]. Gut microbiota plays an essential role in host metabolism [84-86]. In addition, the intestinal microflora is linked to the immune system of the host [87-89]. Owing to this, diseases may be induced in the host depending on whether the intestinal microbiota is healthy, which further affects the overall health of the host.

Inflammatory bowel disease (IBD) is a severe chronic inflammatory disorder of the digestive tract. IBD causes pain and discomfort and is difficult to treat. IBD is classified into two major subtypes: ulcerative colitis (UC) and Crohn's disease (CD) [90-94]. The number of patients with IBD has increased [95-98]. Research to identify the cause behind it is being actively conducted. However, the precise etiology of IBD remains unclear [99].

IBD is caused by a combination of genetic and environmental factors that alter the gut microbiota. Therefore, understanding and identifying the changes in the intestinal microbiota can help ameliorate and treat the symptoms of IBD [90, 100, 101]. In patients with IBD, the intestinal microbial balance is disturbed, and the microbial diversity is reduced [102-105]. At the genus level, Bacteroides, Prevotella, and Ruminococcus are present in a high

ratio and considered healthy intestinal microflora [47, 66, 106]. In patients with IBD, the number of Escherichia coli is increased. Also, it is known that a change in the Firmicutes/Bacteroidetes (F/B) ratio is related to dysbiosis [107-109], but the F/B ratio is characteristically decreased in IBD patients [78, 110, 111]. *Faecalibacterium prausnitzii* (a major species of *Clostridium lectum*) was markedly reduced, which is the most characteristic feature of patients with CD [112-114].

IBD can be treated by changing the unhealthy gut microbiome. Fecal microbiota transplantation (FMT) is currently known to be a very effective treatment strategy for IBD because it transforms the intestinal microflora from an abnormal state into a healthy state. The gut microbiome consists of microbes. They may have side effects because some microorganisms remain unknown. The complex ecosystem of human fecal contents can trigger unexpected adverse effects and cause an unpredictable risk to life. Therefore, we hypothesized a method to alleviate intestinal imbalance through transplantation using well-known microbes.

II. MATERIALS AND METHODS

1. Preparation of Major Gut microbes among Koreans (MGMK) and culture condition

Out of 12 strains, obligate anaerobes comprising the MGMK were cultivated under obligate anaerobic conditions at 90% N2, 5% CO2, and 5% H2 using an anaerobic chamber (Coy System). The facultative anaerobic strains *Escherichia coli* (*E. coli*) and two Lactobacillus strains were cultivated under aerobic conditions. The anaerobes were routinely cultured in Gifu anaerobic media broth (Kisan Bio, Korea) at 37 ℃ for 2−3 days. Anaerobic media were substituted for 3 days in an anaerobic chamber before use to remove oxygen. Lactobacillus strains (*Lactobacillus acidophilus* and *Lactobacillus brevis*) were grown in MRS medium (BD) at 37 ℃ under aerobic conditions, without shaking, for 2 days. *E. coli* was grown in Luria−Bertani broth (10 g/L tryptone, 10 g/L NaCl, and 5 g/L yeast extract) at 37 ℃ under aerobic conditions.

2. MGMK transplantation

MGMK was implanted into mice with colitis by dextran sulfate sodium (DSS). Twelve MGMK strains were inoculated with the same number of bacteria. In the case of germ-free (GF) mice, a mixture was made after adjusting the total bacterial load of each strain to approximately 10^7, and the mice were inoculated. The strain was transplanted using oral gavage. The inoculation volume was adjusted to 200 μl. For specific pathogen-free (SPF) experiment, each strain was inoculated in an amount of approximately 10^9. Among the MGMK strains used in the experiment, all experiments were performed only in an anaerobic chamber for obligate anaerobic strains. Until the transplantation of the strain into mice, all operations were performed in an anaerobic chamber, except for oral gavage, to minimize contact with oxygen.

3. Animals and DSS treatment

GF and SPF mice were used in the experiment. In the GF mouse experiment, BALB/C mice were used. In the SPF mouse experiment, the experiments were performed using mice with a C57BL/6 genetic background. For the mice used in Fig 2.1, GF mice of BALB/C were used. The mice were approximately 7−8 weeks old. Both males and females were used in the experiment. In the experiment using GF mice, care was taken to maintain the GF state of the mice using isocages (Tecniplast Inc., Italy). Before starting the experiment, feces was used to confirm the intestinal microflora of GF mice. It was confirmed that the GF state was established. In all experiments, except the one shown in Fig 2.1, C57BL/6 mice were used. In all experiments, male mice of about 8 weeks were used. GF mice were obtained from Yonsei University College of Mice Breeding at the Medicine GF Mouse Facility. SPF mice were purchased from Orient Bio (Sungnam, Korea). All animal experiments were performed according to the guidelines of the Department of Animal Resources of the Yonsei Biomedical Research Institute.

For the colitis mouse model experiment, dextran sulfate sodium (DSS) was used to obtain colitis-induced mice. Eight-week-old male mice were treated with 2.5% DSS (MP bio) for 5 days to induce colitis; the tap water provided was cut off, and only DSS water was provided. DSS was prepared at a concentration of 2.5% in autoclaved tap water and administered to the mice as drinking water.

4. DAI (Disease Associated Index)

The status of the mice was recorded daily during the administration of DSS. The DAI score was used to indicate the status of the mice, which changed every day. The DAI score was measured according to the degree of decrease in body weight, how watery the stool was, and whether blood was observed in the feces or rectum. Each of these three characteristics was scored and summed to represent the DAI score. The DAI score is calculated as follows: (loss of body weight) + (stool consistency) + (bleeding) = DAI score. (a) Loss of body weight: 0 = none ; 1 = 1–5%; 2 = 6–10%; 3 = 11–18%; 4 = > 18% (b) stool consistency: 0 = normal stool; 1 = soft but still formed; 2 = soft; 3 = very soft or wet; 4 = watery (c) bleeding: 0 = normal; 1 = brown stool; 2 = slightly bloody; 3 = bleeding; 4 = gross rectal bleeding [115].

5. 16s rRNA amplicon sequencing analysis

The extraction method for bacterial DNA was performed using a PowerMax Soil DNA Isolation Kit (MO BIO). Each sequenced sample was prepared according to the Illumina 16S Metagenomic Sequencing Library protocols to amplify the V3 and V4 regions (519F-806R). The DNA quality was measured by PicoGreen and Nanodrop. Input gDNA (10 ng) was PCR amplified. The barcoded fusion primer sequences used for amplifications were as follows: 341F: 5′-CCTACGGGNGGCWGCAG, and 806R: 5′-GACTACHVGGGTATCTAATCC. The final purified product was then quantified using qPCR according to the qPCR Quantification Protocol Guide (KAPA Library Quantification kits for Illumina Sequencing platforms) and qualified using a LabChip GX HT DNA High Sensitivity Kit (PerkinElmer, MA, USA). Paired-end (2 × 300 bp) sequencing was performed by Macrogen using the MiSeq™ platform (Illumina, San Diego, CA, USA). For species identification, sequenced reads were aligned using blast and NCBI 16S microbial database (version downloaded 2018.01.14). Taxonomy information was assigned only to OTUs that met both query coverage > 85% and identity percent > 85%. OTUs that did not meet these two criteria were left unassigned. In general, microbial species was identified with ~ 99% identity with a reference sequence.

6. Statistical analysis

The results obtained in this study were expressed as the mean and standard deviation for each experimental group. Unpaired Student's *t*-test was used to determine the significance between the experimental groups. ($p < 0.05$), with a statistically significant difference between the experimental groups ($p < 0.05$).

III. RESULTS

1. FMT by selecting 12 representative strains of the Korean intestinal microbiota

We constructed a consortium using a well-known strain considering that it existed in many people and has been studied in depth. We also selected strains that were predominantly present in the gut microbiota of Koreans. We selected bacteria at the species level after classifying the distribution of the intestinal microflora of Koreans at the phylum level.

Subsequently, a consortium was created by selecting 12 strains (Table 2), which we called the MGMK. The consortium of 12 strains consisted of bacteria that have been verified to some extent. The harmfulness of the strain was also revealed through various studies on each strain.

We observed how the strains of the MGMK consortium competed for colonization. To elucidate the colonization capability of the 12 strains, GF mice unaffected by other intestinal microorganisms were used. Thus, it was possible to confirm the interaction of each strain without being affected by other external conditions.

At the beginning of this experiment, it was confirmed that the 12 strains between 12 h and 1 day colonized with almost similar occupancy until the 33rd day. After inoculating each strain into mice, the colonization distribution of the 12 strains at the beginning of the experiment was maintained until the end of 33 days. Herein, we identified strains with strong colonization ability (Fig. 2.1). Our results showed that the three strains, *Bacteroides thetaiotaomicron, Bacteroides uniformis,* and *Ruminococcus faecis*, each had a strong colonization ability, although there was a difference in their colonized portion.

We named these three strains SIC3 (Strong Intestinal Colonizer 3). Initially, *E. coli* was

present along with the SIC3 strain. During the experiment, it was confirmed that *E. coli* disappeared, and only the SIC3 strain was predominant. As a result, the stability of the intestinal microbiota was induced.

Phylum	No.	Species	Strain	Genbank accession
Bacteroides	1	*Bacteroides thetaiotaomicron Distaso (1912)*	KCTC 5723	GCF_000011065.1
	2	*Bacteroides uniformis*	KCTC 5204	GCF_000154205.1
	3	*Prevotella melaninogenica*	KCTC 5457	GCF_000144405.1
Firmicutes	4	*Clostridium scindens*	KCTC 5591	GCF_000154505.1
	5	*Clostridium orbiscindens*	KCTC 5970	GCF_000239295.1
	6	*Eubacterium rectale*	KCTC 5835	GCA_000020605.1
	7	*Ruminococcus faecis*	KCTC 5757	NZ_GG697149.2
	8	*Faecalibacterium prausnitzii*	DSM 17677	GCF_001312505.1
	9	*Lactobacillus brevis*	KCTC 3498	GCF_000014465.1
	10	*Lactobacillus acidophilus*	KCTC 3164	GCF_001433895.1
Proteobacteria	11	*Escherichia coli*	KCTC 2441	GCF_000690815.1
Actinobacteria	12	*Bifidobacterium longum sub. Infantis*	KCTC 3249	GCF_000020425.1

Table 2. List of commensal microbes in MGMK (Major Gut Microbes among Koreans) consortium. Strains were selected based on Bacteroides, Firmicutes, Proteobacteria, and Actinobacteria, which are abundant in the intestines of Koreans.

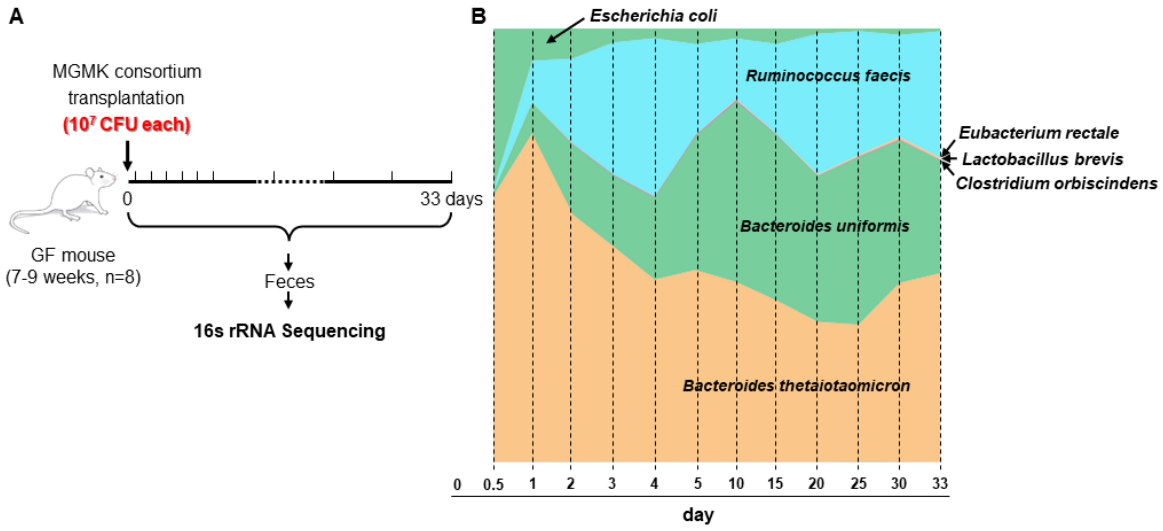

Figure 2.1. Colonization for 33 days after MGMK transplantation into germ-free mice.

a) This is an experimental scheme for transplantation of the MGMK strain quantified in the same amount in GF mice. Feces were harvested 33 days after transplantation and 16S rRNA sequencing was performed using this. b) Microorganisms present in feces for 33 days were profiled.

2. SIC3 alleviated Ulcerative-Colitis in the DSS-induced colitis model

We confirmed the efficacy of the SIC3 consortium in the treatment of IBD. We confirmed that the SIC3 strain was a strong colonizer. Therefore, we investigated whether SIC3 alleviates DSS-induced inflammation. Over time, the DAI score of the SIC3-treated group was much lower than that of the PBS group (Fig 2.2B). Since the DAI score is an indicator of the body weight of the mouse, degree of diarrhea, and bleeding [115], it is safe to say that it reflects the overall condition of the mouse. In the experiment confirming body weight change, it was also proven that the group administered with SIC3 recovered faster than the group treated with PBS (Fig 2.2C). Among colitis-induced mice who lost weight due to diarrhea and showed difficulty in nutrient intake, mice who lost more than a particular weight died. The weight change data were statistically significant. There was a difference in colon length between the SIC3-treated and PBS-treated groups. Shortened colons were observed in DSS-treated mice. This shortened colon length was maintained in the PBS-treated group. In contrast, in mice treated with SIC3, the colon length recuperated to that of normal mice (Fig. 2.3A, B). Symptoms of colitis induced by DSS were alleviated in mice treated with SIC3. Mice in the group treated with SIC3 were more active than those treated with PBS. Grooming was also increased, showing that the hair condition of the SIC3 treatment group was better.

In addition, as a result of histological confirmation of changes in colon tissue through H&E staining, it was identified that the colon tissue of mice administered with SIC3 was close to normal (Fig. 2.3C). It was confirmed that the epithelial layer was recovered by SIC3 treatment. The shape of the goblet cells became normal. In addition, the infiltration of immune cells was reduced compared with that in the PBS-treated group.

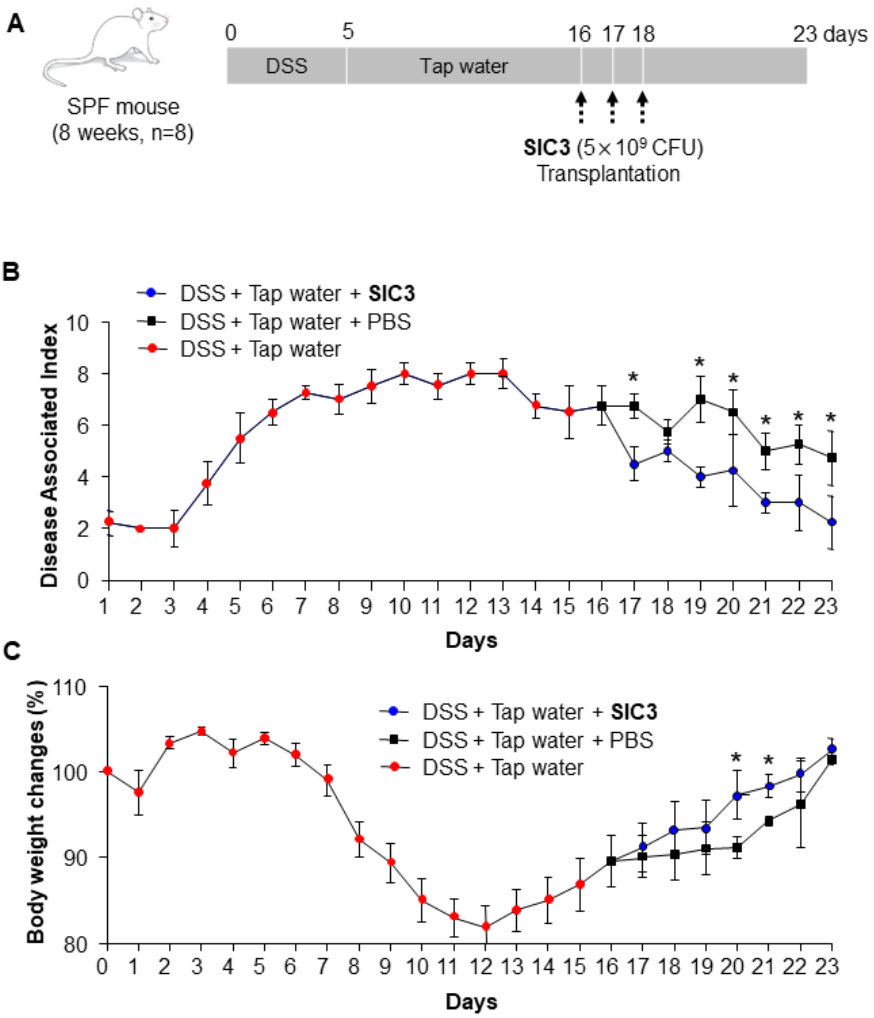

Figure 2.2. SIC3 treatment alleviates DSS-induced colitis. SPF mice were administered with 2.5% DSS and treated with SIC3. a) Schematic diagram of experiment process. After administering 2.5% DSS with tap water, the SIC3 strain was inoculated at 5×10^9 CFU/ml at a specific time point. Transplantation was performed with 200 µl by oral gavage. b) After feeding DSS for 5 days, SIC3 was administered and the condition of the mice observed

was expressed using the DAI score. *$P < 0.05$ vs. DAI score of SIC3 treated or PBS treated. c) The change in weight of mice during the process of administering SIC3 after feeding DSS through drinking water is shown. *$P < 0.05$ vs. change in body weight of SIC3 treated or PBS treated.

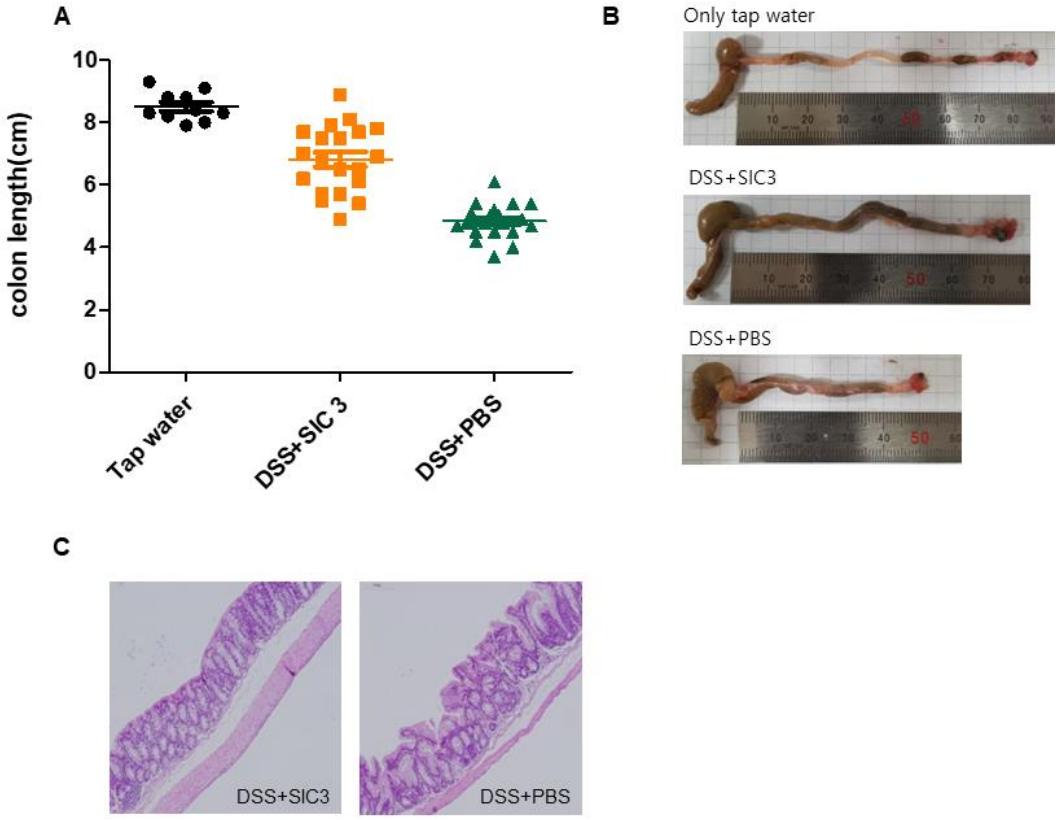

Figure 2.3. The shortened colon length is restored by SIC3 administration. a) Changes in colon length after SIC3 transplantation after DSS treatment. The group treated only with tap water (n=10), the group treated with SIC3 after DSS administration (n=20), and the group treated with PBS after DSS administration (n=20). b) The change in colon length is shown as an image. c) H&E staining image of the colon tissue of a mouse treated with PBS and SIC3 after DSS treatment.

3. SIC3 treatment induced changes in gut microbiota in the colitis model

We hypothesized that these results were due to changes in the gut microbiota. Because of this characteristic of these three strains, it was believed that changes in the gut microbiota alleviated DSS-induced colitis. To validate this, it was necessary to determine whether transplanted SIC3 colonized the intestine. After the transplantation of SIC3, the presence of each strain in the intestine was evaluated using quantitative real-time PCR (Fig. 2.4A). Each SIC3 strain was inoculated in the same amount. The total amount of *B. thetaiotaomicron* was quantitatively measured. Accordingly, we confirmed that the total amount of *B. thetaiotaomicron* added at the beginning remained constant over time. In the case of *B. uniformis*, although the relative number of inoculated bacteria changed, the amount remained similar over time. In *R. faecis*, a relatively small amount was colonized compared with *B. thetaiotaomicron* and *B. uniformis*. Although the number of colonizing bacteria was different for each strain, we demonstrated that all three bacteria could settle in the intestine. The above data support the idea that microbiota changes were induced by SIC3 treatment inoculated with dysbiosis-induced intestinal microflora. This change alleviated the symptoms of colitis. After SIC3 treatment, the SIC3 strains were artificially added from the outside, and the intestinal microbial flora became an environment in which the strains could colonize through any interaction. Therefore, we considered it necessary to identify what changes occurred in the intestinal microflora due to the transplantation of SIC3. We tested the composition of the gut microflora using 16S rRNA sequencing to determine the changes in the gut microbiota. Notably, the group treated with SIC3 showed more diverse gut microflora than the PBS-treated group (Fig. 2.4B). Considering that the most prominent characteristic of the intestinal microflora in dysbiosis and symbiosis is a change in the diversity of the gut microbiota, the increase in the diversity of the gut

microbiota after SIC3 treatment is an encouraging result. It was proven that the intestinal microflora of the SIC3 treatment group became healthier than that of the PBS treatment group. Comparing each strain, the abundance of *Akkermansia muciniphila* decreased, *Muribaculum intestinale* increased, and inoculated *B. thetaiotaomicron* and *B. uniformis* increased in the SIC3 group. In contrast, in the PBS-treated group, it was observed that *A. muciniphila* and *Bacteroides caccae* were present in a high portion of the gut microbial flora. The diversity of bacteria was reduced compared with the SIC3 treated group. During SIC3 colonization, the entire intestinal microbial flora also changed. This change eventually resulted in the alleviation of colitis symptoms.

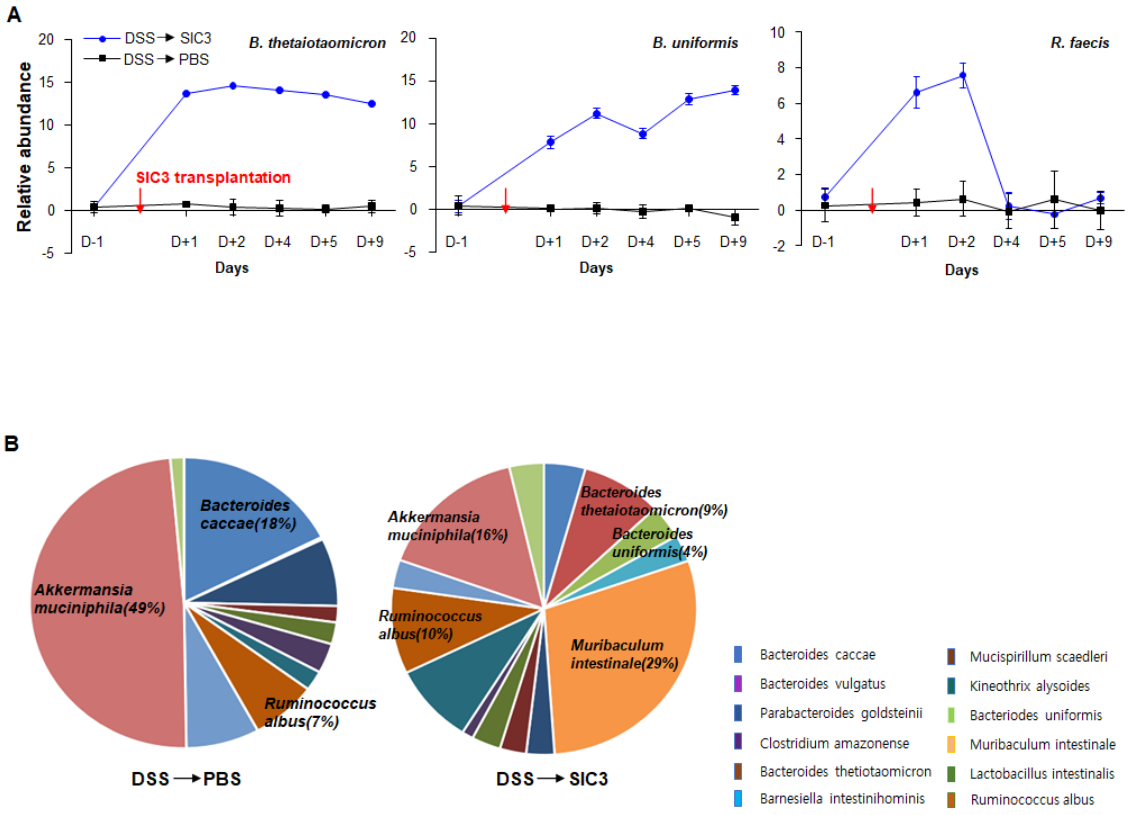

Figure 2.4. The distribution of intestinal microbiota was changed by SIC3 treatment.

a) SIC3 was inoculated after DSS administration, it was confirmed by qRT-PCR how the three strains of SIC3 colonized the intestine. After SIC3 inoculation, feces were harvested and quantitatively measured using feces. b) After DSS treatment, the distribution of microorganisms in the feces of the groups treated with PBS and SIC3 was analyzed for composition through 16S rRNA sequencing.

4. Single treatment of each SIC3 strain cannot alleviate colitis symptoms

To elucidate its capability as a single strain, we examined whether each strain influenced the alleviation of colitis by inoculating it alone. When each strain was administered individually, as shown in Fig. 2.5, 2.6, and 2.7, there was no difference in the DAI score, body weight, or colon length. This result suggests that although each of the SIC3 strains has a strong colonization ability, it does not show any effect when administered as a single treatment. However, colitis symptoms were effectively alleviated when the three strains were combined.

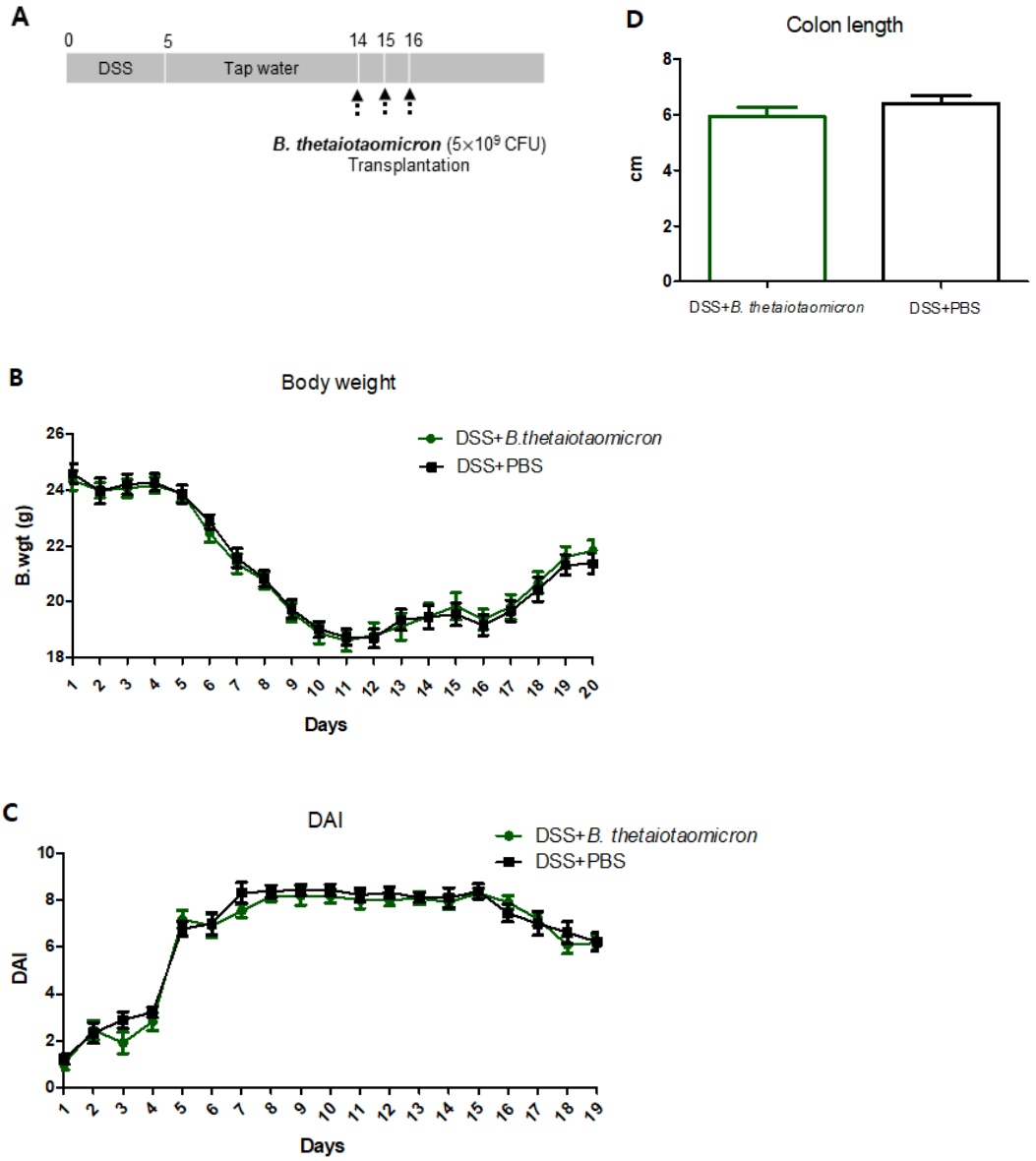

Fig 2.5) Mono-administration of *Bacteroides thetaiotaomicron* does not relieve the symptoms of colitis

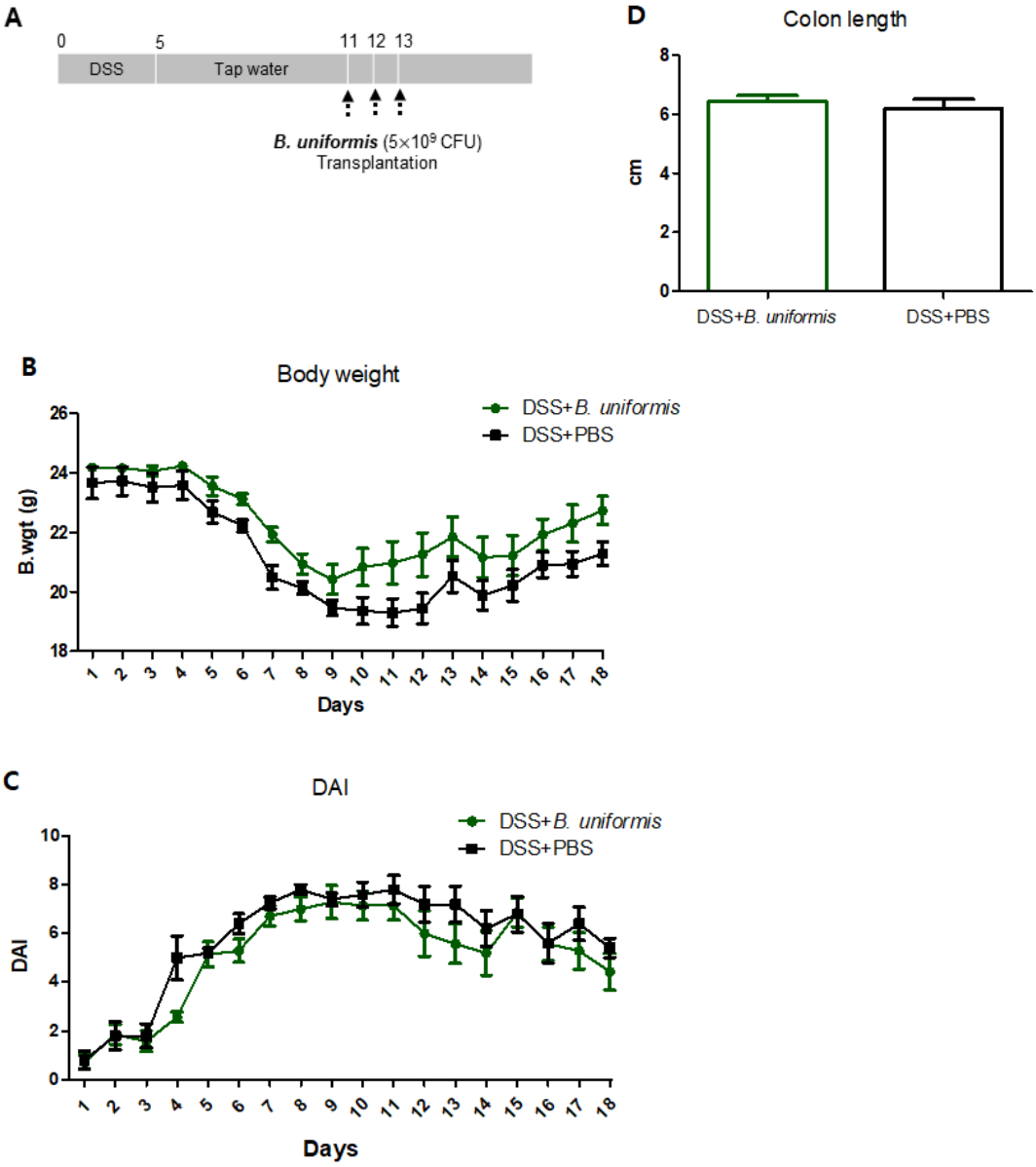

Fig 2.6) Mono-administration of *Bacteroides uniformis* does not relieve the symptoms of colitis

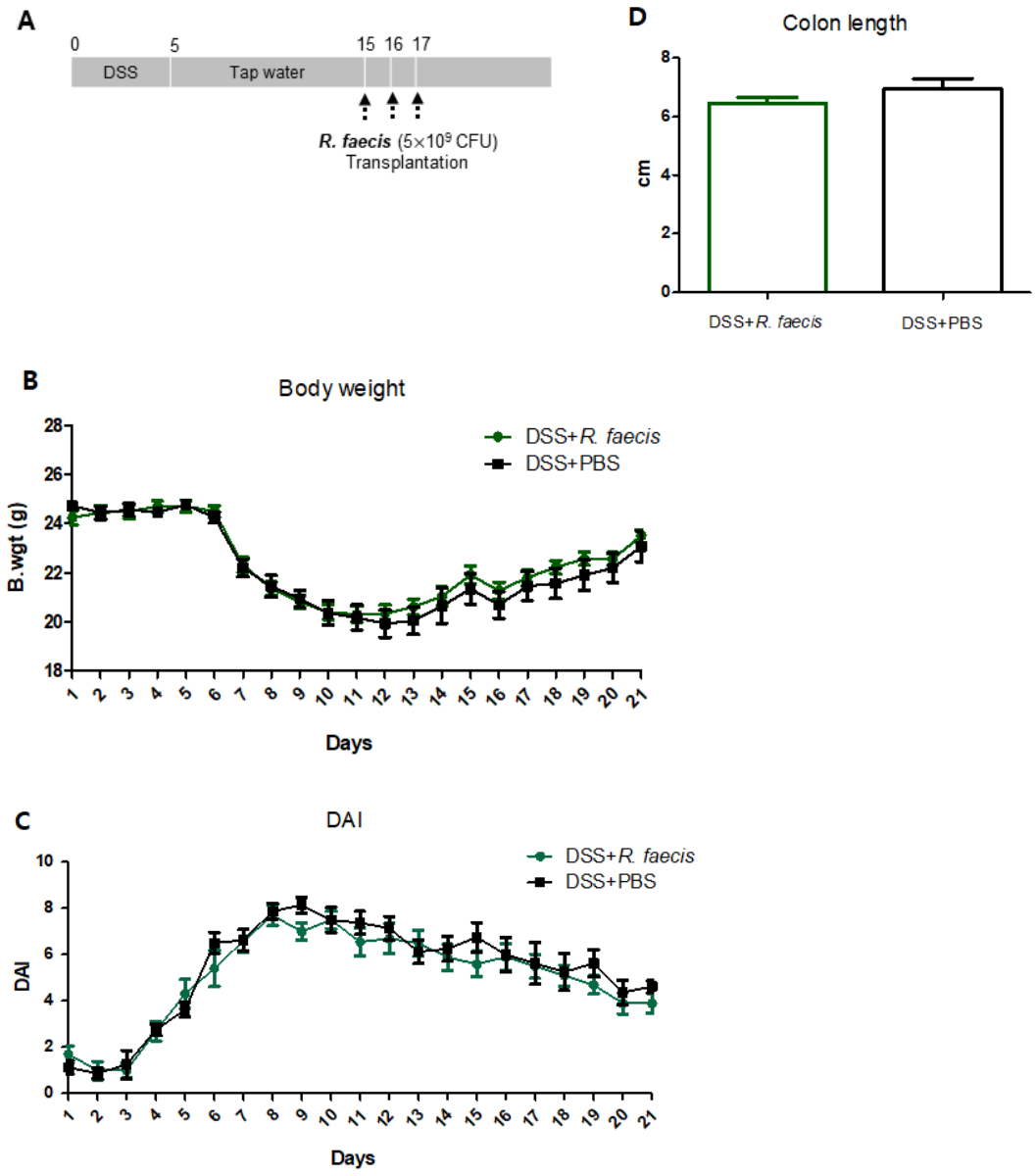

Fig 2.7) Mono-administration of *Ruminococcus faecis* does not relieve the symptoms of colitis

IV. DISCUSSION

Gut microbes play an important role for the host, and numerous studies have reported that owing to this reason, these microbes are associated with various disease [116-119]. Recently, the concept of treating diseases using specific microbes present in the gut microbiome has been emerging in a number of studies. The FMT (Fecal Microbiota Transplantation) method, which helps convert the unhealthy or disrupted state of gut microbiota caused by dysbiosis into a healthy and balanced state, has been used to treat inflammatory bowel disease (IBD). Specifically, FMT is a major treatment for *Clostridiium difficile* infection [120-124]. The number of patients with IBD has been gradually increasing in various regions including Europe, and Asia. The age of patients with IBD has also been decreasing, and the progression of IBD to chronic diseases has led to an increase in their prevalence. Although the most effective treatment of IBD is FMT, it is accompanied by various side effects. Hence, our study examined strategies to reduce such side effects.

A bacterial consortium was generated using a new strain. The bacterial strains which belong to this consortium have been extensively studied and are abundant in the Korean population. We selected these strains because of the rich information available that can allow us to understand their characteristics and hazards. We tested this consortium using germ-free mice and examined how each strain interacts with the other. This allowed us to screen the strains that can dominate colonization against other competing strains. The selected three strains were *Bacteroides thetaiotaomicron, Bacteroides uniformis,* and *Ruminococcus faecis*.

The major strain used to treat IBD is *B. thetaiotaomicron*. It plays a crucial role in Crohn's disease, which is one type of IBD. Although *B. thetaiotaomicron* is known as a

symbiotic gut bacterium associated with IBD, the exact mechanism behind its effect remains undetermined. However, the *B. thetaiotaomicron* strain is known to be critical for protection against weight loss and reduction in colon length and expression of inflammatory markers that are the commonly observed symptoms in a colitis model [125, 126]. Furthermore, it has been reported that *B. thetaiotaomicron* reduces inflammation inside the colon by promoting anti-inflammatory Treg/Th2 cell differentiation and inhibiting the differentiation of Th1/Th17 cells [127]. *Faecalibacterium prausnitzii* is most widely known among the bacteria commonly used to alleviate colitis [128-131]. *F. prausnitzii* is reported to be largely deficient in patients with IBD [132]. Experimental results using *F. prausnitzii* showed that its supernatant reduced inflammation by inhibiting Th17 differentiation and reducing IL-6 expression in a DSS-induced colitis model [133, 134].

We aimed to alleviate IBD using the strong colonization ability of the SIC 3 strains. Similar to single treatment of *B. thetaiotaomicron* or use of *F. prausnitzii* supernatant, we predicted that strong colonization of the SIC3 strains would alter gut microbiota and alleviate gut dysbiosis, enabling the treatment of colitis.

The most prominent characteristic of gut microbiota under dysbiosis is the decrease in microbial community diversity [135]. Although changes in distribution of beneficial and harmful bacteria are another important characteristic of dysbiosis, we focused on the changes in microbial community diversity influenced by SIC3 based on the notion of using superior dominance of MGMK to regulate the balance of gut microbiome. The results of 16S rRNA analysis (Fig. 2.4) showed that administration of SIC3 increased the diversity of gut microbiota. In addition, some microbiota, such as *Akkermansia muciniphila, Bacteroides caccae and Muribaculum intestinale* showed characteristics of either increase or decrease. *A. muciniphila* was decreased by one-third in the SIC3-administered group. *A. muciniphila* is a bacterial strain that hydrolyzes mucin present in the gut epithelial cells

and uses the obtained product. In the process, it secondarily produces acetic acid and propionic acid. In addition, *A. muciniphila* shows a tendency of decrease in patients with IBD as well as in those with metabolic disorders such as obesity and diabetes. Although more studies are required to understand the decrease in this bacterial strain upon SIC3 administration given its reported anti-inflammatory function, the fact that it appeared in the process of increased diversity of gut microbiota suggests its contribution to the alleviation of dysbiosis. Next, the *B. caccae* strain was present at a high percentage in the control group, but it showed a rapid decrease in the SIC3-administered group. *B. caccae* is known as a pathogenic bacterium present in gut microbiota of patients with IBD. The decrease in such pathogens in the group treated with SIC3 indicates a reduction in dysbiosis. Finally, *M. intestinale* was largely increased in the group treated with SIC3. Knowledge on *M. intestinale* is scarce, other than the fact that it is an anaerobic bacterium present in the intestine. More studies are needed to understand the cause of increase in *M. intestinale*.

The fact that the increase in diversity shown in the 16S rRNA data was induced by the SIC3 strains that were transplanted was validated by qRT-PCR (Fig. 2.4). The qRT-PCR result showed that the three strains transplanted into the intestine were dominant for a certain period of time. In other words, the exogenous SIC3 strains securely settled in the intestine and induced changes in overall gut microbiome. Such changes led to a healthy state of the gut microbiome with reduced dysbiosis. Furthermore, the fact that transplanted SIC3 alleviated weight loss as well as shortening of colon length and restored DAI score indicates that SIC3 treatment may also alleviate symptoms of colitis in addition to improving gut microbiota. Furthermore, H&E staining revealed the restoration of gut epithelial cells. The most important factor for symptom displays in the colitis model induced by DSS is the induction of rapid inflammatory responses by migration of exogenous microorganisms, which exist in the lumen, towards the lamina propria owing to

damage to large intestinal epithelial cells by DSS. The group treated with SIC3 showed a certain level of restoration in the damaged gut epithelial cells compared to that in the control group. This clearly indicates alleviation of colitis and confirms that the SIC3 strains are involved in the restoration of gut epithelial cells.

Although each strain of SIC3 exerted strong dominance, single administration of each strain did not show the same effects. We speculated that the strong dominance of each strain would reduce gut dysbiosis and alleviate colitis, and therefore, expected that a single strain would achieve a certain level of symptom alleviation. However, administration of a single strain did not show any effect, indicating that all three strains need to be present and the interaction among these strains leads to alleviation of DSS-induced colitis symptoms. Although the exact interactions among the three strains were not elucidated, we demonstrated that their interactions are beneficial for reducing gut dysbiosis. Examining these interactions will allow SIC3 to be a more effective therapeutic agent.

V. CONCLUSION

We identified SIC3 strains using the MGMK consortium. It was confirmed that IBD was alleviated by the three strains with excellent colonization ability. We demonstrated that the SIC3 strain we put into the intestine properly colonized and induced a change in the intestinal microbial flora, making it healthy. In addition, as a result of treatment with SIC3 in the DSS-induced colitis mouse model, symptoms were relieved. It was confirmed that the shortened colon length was restored. We demonstrated that the alleviation of IBD was possible in a mouse model using SIC3.

REFERENCES

1. Yoon, M.Y., et al., *A single gene of a commensal microbe affects host susceptibility to enteric infection.* Nat Commun, 2016. 7: p. 11606.
2. Hsiao, A., et al., *Members of the human gut microbiota involved in recovery from Vibrio cholerae infection.* Nature, 2014. 515(7527): p. 423-6.
3. Midani, F.S., et al., *Human Gut Microbiota Predicts Susceptibility to Vibrio cholerae Infection.* J Infect Dis, 2018. 218(4): p. 645-653.
4. Zhao, W., et al., *Antagonism toward the intestinal microbiota and its effect on Vibrio cholerae virulence.* Science, 2018. 359(6372): p. 210-213.
5. Yurist-Doutsch, S., et al., *Gastrointestinal microbiota-mediated control of enteric pathogens.* Annu Rev Genet, 2014. 48: p. 361-82.
6. McKenney, P.T. and E.G. Pamer, *From Hype to Hope: The Gut Microbiota in Enteric Infectious Disease.* Cell, 2015. 163(6): p. 1326-32.
7. Kamada, N., et al., *Role of the gut microbiota in immunity and inflammatory disease.* Nat Rev Immunol, 2013. 13(5): p. 321-35.
8. Schmidt, T.S.B., J. Raes, and P. Bork, *The Human Gut Microbiome: From Association to Modulation.* Cell, 2018. 172(6): p. 1198-1215.
9. Anderson, M.C., et al., *Shigella sonnei Encodes a Functional T6SS Used for Interbacterial Competition and Niche Occupancy.* Cell Host Microbe, 2017. 21(6): p. 769-776.e3.
10. Kommineni, S., et al., *Bacteriocin production augments niche competition by enterococci in the mammalian gastrointestinal tract.* Nature, 2015. 526(7575): p. 719-22.
11. García-Bayona, L. and L.E. Comstock, *Bacterial antagonism in host-associated microbial communities.* Science, 2018. 361(6408).

12. Dethlefsen, L., et al., *The pervasive effects of an antibiotic on the human gut microbiota, as revealed by deep 16S rRNA sequencing.* PLoS Biol, 2008. 6(11): p. e280.
13. Russell, S.L., et al., *Perinatal antibiotic-induced shifts in gut microbiota have differential effects on inflammatory lung diseases.* J Allergy Clin Immunol, 2015. 135(1): p. 100-9.
14. Gasparrini, A.J., et al., *Antibiotic perturbation of the preterm infant gut microbiome and resistome.* Gut Microbes, 2016. 7(5): p. 443-9.
15. Dethlefsen, L. and D.A. Relman, *Incomplete recovery and individualized responses of the human distal gut microbiota to repeated antibiotic perturbation.* Proc Natl Acad Sci U S A, 2011. 108 Suppl 1(Suppl 1): p. 4554-61.
16. Sprinz, H., et al., *The response of the germfree guinea pig to oral bacterial challenge with Escherichia coli and Shigella flexneri.* Am J Pathol, 1961. 39(6): p. 681-95.
17. Sekirov, I., et al., *Antibiotic-induced perturbations of the intestinal microbiota alter host susceptibility to enteric infection.* Infect Immun, 2008. 76(10): p. 4726-36.
18. Buffie, C.G., et al., *Profound alterations of intestinal microbiota following a single dose of clindamycin results in sustained susceptibility to Clostridium difficile-induced colitis.* Infect Immun, 2012. 80(1): p. 62-73.
19. Theriot, C.M., et al., *Antibiotic-induced shifts in the mouse gut microbiome and metabolome increase susceptibility to Clostridium difficile infection.* Nat Commun, 2014. 5: p. 3114.
20. Ubeda, C., et al., *Vancomycin-resistant Enterococcus domination of intestinal microbiota is enabled by antibiotic treatment in mice and precedes bloodstream invasion in humans.* J Clin Invest, 2010. 120(12): p. 4332-41.

21. Vogt, S.L., J. Peña-Díaz, and B.B. Finlay, *Chemical communication in the gut: Effects of microbiota-generated metabolites on gastrointestinal bacterial pathogens.* Anaerobe, 2015. 34: p. 106-15.
22. Ng, K.M., et al., *Microbiota-liberated host sugars facilitate post-antibiotic expansion of enteric pathogens.* Nature, 2013. 502(7469): p. 96-9.
23. Jump, R.L., et al., *Metabolomics analysis identifies intestinal microbiota-derived biomarkers of colonization resistance in clindamycin-treated mice.* PLoS One, 2014. 9(7): p. e101267.
24. Lee, K.M., et al., *Activation of cholera toxin production by anaerobic respiration of trimethylamine N-oxide in Vibrio cholerae.* J Biol Chem, 2012. 287(47): p. 39742-52.
25. Oh, Y.T., et al., *Cholera toxin production during anaerobic trimethylamine N-oxide respiration is mediated by stringent response in Vibrio cholerae.* J Biol Chem, 2014. 289(19): p. 13232-42.
26. Yoon, S.S. and J.J. Mekalanos, *2,3-butanediol synthesis and the emergence of the Vibrio cholerae El Tor biotype.* Infect Immun, 2006. 74(12): p. 6547-56.
27. Ohashi, Y., et al., *Depiction of metabolome changes in histidine-starved Escherichia coli by CE-TOFMS.* Mol Biosyst, 2008. 4(2): p. 135-47.
28. Ooga, T., et al., *Metabolomic anatomy of an animal model revealing homeostatic imbalances in dyslipidaemia.* Mol Biosyst, 2011. 7(4): p. 1217-23.
29. Sugimoto, M., et al., *Capillary electrophoresis mass spectrometry-based saliva metabolomics identified oral, breast and pancreatic cancer-specific profiles.* Metabolomics, 2010. 6(1): p. 78-95.
30. Caballero, S., et al., *Cooperating Commensals Restore Colonization Resistance to Vancomycin-Resistant Enterococcus faecium.* Cell Host Microbe, 2017. 21(5): p. 592-602.e4.

31. Sekirov, I. and B.B. Finlay, *The role of the intestinal microbiota in enteric infection.* J Physiol, 2009. 587(Pt 17): p. 4159-67.
32. Chua, K. and B.P. Howden, *Treating Gram-positive infections: vancomycin update and the whys, wherefores and evidence base for continuous infusion of anti-Gram-positive antibiotics.* Curr Opin Infect Dis, 2009. 22(6): p. 525-34.
33. Hecht, D.W., *Prevalence of antibiotic resistance in anaerobic bacteria: worrisome developments.* Clin Infect Dis, 2004. 39(1): p. 92-7.
34. Lusk, R.H., et al., *Gastrointestinal side effects of clindamycin and ampicillin therapy.* J Infect Dis, 1977. 135 Suppl: p. S111-9.
35. Douglas, R.L. and J.W. Kislak, *Treatment of Bacteroides fragilis bacteremia with clindamycin.* J Infect Dis, 1973. 128(4): p. 569-71.
36. Tomioka, S. and Y. Kobayashi, *[Bacteriological studies on Bacteroides fragilis infections and treatment with clindamycin for intravenous injection (author's transl)].* Jpn J Antibiot, 1977. 30(1): p. 30-5.
37. Hirata, N., et al., *Pretreatment of mice with clindamycin improves survival of endotoxic shock by modulating the release of inflammatory cytokines.* Antimicrob Agents Chemother, 2001. 45(9): p. 2638-42.
38. Kishi, K., et al., *Clindamycin suppresses endotoxin released by ceftazidime-treated Escherichia coli O55:B5 and subsequent production of tumor necrosis factor alpha and interleukin-1 beta.* Antimicrob Agents Chemother, 1999. 43(3): p. 616-22.
39. Nakano, T., et al., *Clindamycin modulates inflammatory-cytokine induction in lipopolysaccharide-stimulated mouse peritoneal macrophages.* Antimicrob Agents Chemother, 2003. 47(1): p. 363-7.
40. Veringa, E.M. and J. Verhoef, *Clindamycin at subinhibitory concentrations enhances antibody- and complement-dependent phagocytosis by human*

polymorphonuclear leukocytes of Staphylococcus aureus. Chemotherapy, 1987. 33(4): p. 243-9.

41. Veringa, E.M., et al., *Enhancement of opsonophagocytosis of Bacteroides spp. by clindamycin in subinhibitory concentrations.* J Antimicrob Chemother, 1989. 23(4): p. 577-87.
42. Sakamoto, M. and Y. Benno, *Reclassification of Bacteroides distasonis, Bacteroides goldsteinii and Bacteroides merdae as Parabacteroides distasonis gen. nov., comb. nov., Parabacteroides goldsteinii comb. nov. and Parabacteroides merdae comb. nov.* Int J Syst Evol Microbiol, 2006. 56(Pt 7): p. 1599-1605.
43. Song, Y., et al., *"Bacteroides goldsteinii sp. nov." isolated from clinical specimens of human intestinal origin.* J Clin Microbiol, 2005. 43(9): p. 4522-7.
44. Rhine, J.A. and R.K. Taylor, *TcpA pilin sequences and colonization requirements for O1 and O139 vibrio cholerae.* Mol Microbiol, 1994. 13(6): p. 1013-20.
45. Umesaki, Y. and H. Setoyama, *Immune responses of mice to orally administered asialo GM1-specific rabbit IgG in the presence or absence of cholera toxin.* Immunology, 1992. 75(2): p. 386-8.
46. Sato, E., et al., *Developmental profiles of glycolipids in mouse small intestine.* J Biochem, 1982. 91(6): p. 2013-9.
47. Arumugam, M., et al., *Enterotypes of the human gut microbiome.* Nature, 2011. 473(7346): p. 174-80.
48. Nagpal, R., et al., *Comparative Microbiome Signatures and Short-Chain Fatty Acids in Mouse, Rat, Non-human Primate, and Human Feces.* Front Microbiol, 2018. 9: p. 2897.
49. Nguyen, T.L., et al., *How informative is the mouse for human gut microbiota research?* Dis Model Mech, 2015. 8(1): p. 1-16.

50. *Structure, function and diversity of the healthy human microbiome.* Nature, 2012. 486(7402): p. 207-14.
51. Dick, L.K., et al., *Host distributions of uncultivated fecal Bacteroidales bacteria reveal genetic markers for fecal source identification.* Appl Environ Microbiol, 2005. 71(6): p. 3184-91.
52. Lange, K., et al., *Effects of Antibiotics on Gut Microbiota.* Dig Dis, 2016. 34(3): p. 260-8.
53. Modi, S.R., J.J. Collins, and D.A. Relman, *Antibiotics and the gut microbiota.* J Clin Invest, 2014. 124(10): p. 4212-8.
54. Bouladoux, N., O.J. Harrison, and Y. Belkaid, *The Mouse Model of Infection with Citrobacter rodentium.* Curr Protoc Immunol, 2017. 119: p. 19.15.1-19.15.25.
55. Deng, H., et al., *Bacteroides fragilis Prevents Clostridium difficile Infection in a Mouse Model by Restoring Gut Barrier and Microbiome Regulation.* Front Microbiol, 2018. 9: p. 2976.
56. Klose, K.E., *The suckling mouse model of cholera.* Trends Microbiol, 2000. 8(4): p. 189-91.
57. Ritchie, J.M., et al., *Back to the future: studying cholera pathogenesis using infant rabbits.* mBio, 2010. 1(1).
58. Angelichio, M.J., et al., *Vibrio cholerae intestinal population dynamics in the suckling mouse model of infection.* Infect Immun, 1999. 67(8): p. 3733-9.
59. Nygren, E., et al., *Establishment of an adult mouse model for direct evaluation of the efficacy of vaccines against Vibrio cholerae.* Infect Immun, 2009. 77(8): p. 3475-84.
60. Sawasvirojwong, S., et al., *An Adult Mouse Model of Vibrio cholerae-induced Diarrhea for Studying Pathogenesis and Potential Therapy of Cholera.* PLoS Negl Trop Dis, 2013. 7(6): p. e2293.

61. Herrington, D.A., et al., *Toxin, toxin-coregulated pili, and the toxR regulon are essential for Vibrio cholerae pathogenesis in humans.* J Exp Med, 1988. 168(4): p. 1487-92.
62. Attridge, S.R., et al., *Detection of antibodies to toxin-coregulated pili in sera from cholera patients.* Infect Immun, 2004. 72(3): p. 1824-7.
63. Krebs, S.J. and R.K. Taylor, *Protection and attachment of Vibrio cholerae mediated by the toxin-coregulated pilus in the infant mouse model.* J Bacteriol, 2011. 193(19): p. 5260-70.
64. Fletcher, C.M., et al., *A general O-glycosylation system important to the physiology of a major human intestinal symbiont.* Cell, 2009. 137(2): p. 321-31.
65. Hooper, L.V., T. Midtvedt, and J.I. Gordon, *How host-microbial interactions shape the nutrient environment of the mammalian intestine.* Annu Rev Nutr, 2002. 22: p. 283-307.
66. Bäckhed, F., et al., *Host-bacterial mutualism in the human intestine.* Science, 2005. 307(5717): p. 1915-20.
67. Rakoff-Nahoum, S., K.R. Foster, and L.E. Comstock, *The evolution of cooperation within the gut microbiota.* Nature, 2016. 533(7602): p. 255-9.
68. Sun, Y. and M.X. O'Riordan, *Regulation of bacterial pathogenesis by intestinal short-chain Fatty acids.* Adv Appl Microbiol, 2013. 85: p. 93-118.
69. Fu, Y., B.T. Ho, and J.J. Mekalanos, *Tracking Vibrio cholerae Cell-Cell Interactions during Infection Reveals Bacterial Population Dynamics within Intestinal Microenvironments.* Cell Host Microbe, 2018. 23(2): p. 274-281.e2.
70. Almagro-Moreno, S. and E.F. Boyd, *Sialic acid catabolism confers a competitive advantage to pathogenic vibrio cholerae in the mouse intestine.* Infect Immun, 2009. 77(9): p. 3807-16.
71. Spagnuolo, A.M., V. Dirita, and D. Kirschner, *A model for Vibrio cholerae*

colonization of the human intestine. J Theor Biol, 2011. 289: p. 247-58.

72. Reddi, G., et al., *Catabolism of mucus components influences motility of Vibrio cholerae in the presence of environmental reservoirs.* PLoS One, 2018. 13(7): p. e0201383.
73. McDonald, N.D., et al., *Host-Derived Sialic Acids Are an Important Nutrient Source Required for Optimal Bacterial Fitness In Vivo.* mBio, 2016. 7(2): p. e02237-15.
74. Ramakrishna, B.S. and V.I. Mathan, *Colonic dysfunction in acute diarrhoea: the role of luminal short chain fatty acids.* Gut, 1993. 34(9): p. 1215-8.
75. Bäumler, A.J. and V. Sperandio, *Interactions between the microbiota and pathogenic bacteria in the gut.* Nature, 2016. 535(7610): p. 85-93.
76. Patra, T., et al., *The Entner-Doudoroff pathway is obligatory for gluconate utilization and contributes to the pathogenicity of Vibrio cholerae.* J Bacteriol, 2012. 194(13): p. 3377-85.
77. Sidhu, M. and D. van der Poorten, *The gut microbiome.* Aust Fam Physician, 2017. 46(4): p. 206-211.
78. Rinninella, E., et al., *What is the Healthy Gut Microbiota Composition? A Changing Ecosystem across Age, Environment, Diet, and Diseases.* Microorganisms, 2019. 7(1).
79. Belizário, J.E. and M. Napolitano, *Human microbiomes and their roles in dysbiosis, common diseases, and novel therapeutic approaches.* Front Microbiol, 2015. 6: p. 1050.
80. Bull, M.J. and N.T. Plummer, *Part 1: The Human Gut Microbiome in Health and Disease.* Integr Med (Encinitas), 2014. 13(6): p. 17-22.
81. Harris, M.A., C.A. Reddy, and G.R. Carter, *Anaerobic bacteria from the large intestine of mice.* Appl Environ Microbiol, 1976. 31(6): p. 907-12.

82. Chen, Y., J. Zhou, and L. Wang, *Role and Mechanism of Gut Microbiota in Human Disease.* Front Cell Infect Microbiol, 2021. 11: p. 625913.
83. Ding, R.X., et al., *Revisit gut microbiota and its impact on human health and disease.* J Food Drug Anal, 2019. 27(3): p. 623-631.
84. Lozupone, C.A., et al., *Diversity, stability and resilience of the human gut microbiota.* Nature, 2012. 489(7415): p. 220-30.
85. Sharma, S. and P. Tripathi, *Gut microbiome and type 2 diabetes: where we are and where to go?* J Nutr Biochem, 2019. 63: p. 101-108.
86. Ley, R.E., et al., *Obesity alters gut microbial ecology.* Proc Natl Acad Sci U S A, 2005. 102(31): p. 11070-5.
87. Huurre, A., et al., *Mode of delivery - effects on gut microbiota and humoral immunity.* Neonatology, 2008. 93(4): p. 236-40.
88. Shi, N., et al., *Interaction between the gut microbiome and mucosal immune system.* Mil Med Res, 2017. 4: p. 14.
89. Takiishi, T., C.I.M. Fenero, and N.O.S. Câmara, *Intestinal barrier and gut microbiota: Shaping our immune responses throughout life.* Tissue Barriers, 2017. 5(4): p. e1373208.
90. Ni, J., et al., *Gut microbiota and IBD: causation or correlation?* Nat Rev Gastroenterol Hepatol, 2017. 14(10): p. 573-584.
91. Gohil, K. and B. Carramusa, *Ulcerative colitis and Crohn's disease.* P t, 2014. 39(8): p. 576-7.
92. Panaccione, R., *Mechanisms of inflammatory bowel disease.* Gastroenterol Hepatol (N Y), 2013. 9(8): p. 529-32.
93. Veauthier, B. and J.R. Hornecker, *Crohn's Disease: Diagnosis and Management.* Am Fam Physician, 2018. 98(11): p. 661-669.
94. Wilkins, T., K. Jarvis, and J. Patel, *Diagnosis and management of Crohn's disease.*

Am Fam Physician, 2011. 84(12): p. 1365-75.

95. Carroll, M.W., et al., *The Impact of Inflammatory Bowel Disease in Canada 2018: Children and Adolescents with IBD.* J Can Assoc Gastroenterol, 2019. 2(Suppl 1): p. S49-s67.

96. Faye, A.S., et al., *Increasing Prevalence of Frailty and Its Association with Readmission and Mortality Among Hospitalized Patients with IBD.* Dig Dis Sci, 2021. 66(12): p. 4178-4190.

97. Kaplan, G.G., *The global burden of IBD: from 2015 to 2025.* Nat Rev Gastroenterol Hepatol, 2015. 12(12): p. 720-7.

98. Kaplan, G.G. and S.C. Ng, *Understanding and Preventing the Global Increase of Inflammatory Bowel Disease.* Gastroenterology, 2017. 152(2): p. 313-321.e2.

99. Dixon, L.J., et al., *Combinatorial effects of diet and genetics on inflammatory bowel disease pathogenesis.* Inflamm Bowel Dis, 2015. 21(4): p. 912-22.

100. Gkouskou, K.K., et al., *The gut microbiota in mouse models of inflammatory bowel disease.* Front Cell Infect Microbiol, 2014. 4: p. 28.

101. Khan, I., et al., *Alteration of Gut Microbiota in Inflammatory Bowel Disease (IBD): Cause or Consequence? IBD Treatment Targeting the Gut Microbiome.* Pathogens, 2019. 8(3).

102. Kriss, M., et al., *Low diversity gut microbiota dysbiosis: drivers, functional implications and recovery.* Curr Opin Microbiol, 2018. 44: p. 34-40.

103. Gong, D., et al., *Involvement of Reduced Microbial Diversity in Inflammatory Bowel Disease.* Gastroenterol Res Pract, 2016. 2016: p. 6951091.

104. Ott, S.J., et al., *Reduction in diversity of the colonic mucosa associated bacterial microflora in patients with active inflammatory bowel disease.* Gut, 2004. 53(5): p. 685-93.

105. Joossens, M., et al., *Dysbiosis of the faecal microbiota in patients with Crohn's*

disease and their unaffected relatives. Gut, 2011. 60(5): p. 631-7.

106. Seksik, P., et al., *Alterations of the dominant faecal bacterial groups in patients with Crohn's disease of the colon.* Gut, 2003. 52(2): p. 237-42.

107. Turnbaugh, P.J., et al., *An obesity-associated gut microbiome with increased capacity for energy harvest.* Nature, 2006. 444(7122): p. 1027-31.

108. Turnbaugh, P.J., et al., *The effect of diet on the human gut microbiome: a metagenomic analysis in humanized gnotobiotic mice.* Sci Transl Med, 2009. 1(6): p. 6ra14.

109. Thaiss, C.A., et al., *Persistent microbiome alterations modulate the rate of post-dieting weight regain.* Nature, 2016. 540(7634): p. 544-551.

110. Stojanov, S., A. Berlec, and B. Štrukelj, *The Influence of Probiotics on the Firmicutes/Bacteroidetes Ratio in the Treatment of Obesity and Inflammatory Bowel disease.* Microorganisms, 2020. 8(11).

111. Mariat, D., et al., *The Firmicutes/Bacteroidetes ratio of the human microbiota changes with age.* BMC Microbiol, 2009. 9: p. 123.

112. Sokol, H., et al., *Analysis of bacterial bowel communities of IBD patients: what has it revealed?* Inflamm Bowel Dis, 2008. 14(6): p. 858-67.

113. Cao, Y., J. Shen, and Z.H. Ran, *Association between Faecalibacterium prausnitzii Reduction and Inflammatory Bowel Disease: A Meta-Analysis and Systematic Review of the Literature.* Gastroenterol Res Pract, 2014. 2014: p. 872725.

114. Jia, W., et al., *Is the abundance of Faecalibacterium prausnitzii relevant to Crohn's disease?* FEMS Microbiol Lett, 2010. 310(2): p. 138-44.

115. Cooper, H.S., et al., *Clinicopathologic study of dextran sulfate sodium experimental murine colitis.* Lab Invest, 1993. 69(2): p. 238-49.

116. Angelucci, F., et al., *Antibiotics, gut microbiota, and Alzheimer's disease.* J Neuroinflammation, 2019. 16(1): p. 108.

117. Mangiola, F., et al., *Gut microbiota in autism and mood disorders.* World J Gastroenterol, 2016. 22(1): p. 361-8.

118. Patterson, E., et al., *Gut microbiota, obesity and diabetes.* Postgrad Med J, 2016. 92(1087): p. 286-300.

119. Schoeler, M. and R. Caesar, *Dietary lipids, gut microbiota and lipid metabolism.* Rev Endocr Metab Disord, 2019. 20(4): p. 461-472.

120. Wang, J.W., et al., *Fecal microbiota transplantation: Review and update.* J Formos Med Assoc, 2019. 118 Suppl 1: p. S23-s31.

121. Blanchaert, C., B. Strubbe, and H. Peeters, *Fecal microbiota transplantation in ulcerative colitis.* Acta Gastroenterol Belg, 2019. 82(4): p. 519-528.

122. Akutko, K. and A. Stawarski, *Probiotics, Prebiotics and Synbiotics in Inflammatory Bowel Diseases.* J Clin Med, 2021. 10(11).

123. Song, J.H. and Y.S. Kim, *Recurrent Clostridium difficile Infection: Risk Factors, Treatment, and Prevention.* Gut Liver, 2019. 13(1): p. 16-24.

124. Khoruts, A. and M.J. Sadowsky, *Understanding the mechanisms of faecal microbiota transplantation.* Nat Rev Gastroenterol Hepatol, 2016. 13(9): p. 508-16.

125. Delday, M., et al., *Bacteroides thetaiotaomicron Ameliorates Colon Inflammation in Preclinical Models of Crohn's Disease.* Inflamm Bowel Dis, 2019. 25(1): p. 85-96.

126. Brown, E.M., et al., *Bacteroides-Derived Sphingolipids Are Critical for Maintaining Intestinal Homeostasis and Symbiosis.* Cell Host Microbe, 2019. 25(5): p. 668-680.e7.

127. Li, K., et al., *Bacteroides thetaiotaomicron relieves colon inflammation by activating aryl hydrocarbon receptor and modulating CD4(+)T cell homeostasis.* Int Immunopharmacol, 2021. 90: p. 107183.

128. Miquel, S., et al., *Faecalibacterium prausnitzii and human intestinal health.* Curr Opin Microbiol, 2013. 16(3): p. 255-61.

129. Kawade, Y., et al., *Administration of live, but not inactivated, Faecalibacterium prausnitzii has a preventive effect on dextran sodium sulfate-induced colitis in mice.* Mol Med Rep, 2019. 20(1): p. 25-32.

130. Zhou, L., et al., *Faecalibacterium prausnitzii Produces Butyrate to Maintain Th17/Treg Balance and to Ameliorate Colorectal Colitis by Inhibiting Histone Deacetylase 1.* Inflamm Bowel Dis, 2018. 24(9): p. 1926-1940.

131. Xu, J., et al., *Faecalibacterium prausnitzii-derived microbial anti-inflammatory molecule regulates intestinal integrity in diabetes mellitus mice via modulating tight junction protein expression.* J Diabetes, 2020. 12(3): p. 224-236.

132. Machiels, K., et al., *A decrease of the butyrate-producing species Roseburia hominis and Faecalibacterium prausnitzii defines dysbiosis in patients with ulcerative colitis.* Gut, 2014. 63(8): p. 1275-83.

133. Huang, X.L., et al., *Faecalibacterium prausnitzii supernatant ameliorates dextran sulfate sodium induced colitis by regulating Th17 cell differentiation.* World J Gastroenterol, 2016. 22(22): p. 5201-10.

134. Zhang, M., et al., *Faecalibacterium prausnitzii inhibits interleukin-17 to ameliorate colorectal colitis in rats.* PLoS One, 2014. 9(10): p. e109146.

135. Petersen, C. and J.L. Round, *Defining dysbiosis and its influence on host immunity and disease.* Cell Microbiol, 2014. 16(7): p. 1024-33.

ABSTRACT(IN KOREAN)

장내 감염과 염증성 장질환에 대한 공생미생물의 유익한 효과

<지도교수 윤상선>

연세대학교 대학원 의과학과

유진선

장내 미생물은 숙주의 건강상태와 밀접하게 연관되어 있다. 그렇기 때문에 장내 미생물 균총의 균형이 유지된다는 것은 숙주가 건강한 상태를 유지하는데 있어서 매우 중요한 역할을 한다. 어떠한 이유에 의해서 이러한 장내미생물 균총의 균형이 깨지게 되면, 우리는 이를 dysbiosis 라고 부른다. Dysbiosis 상태에서는 외부의 병원성 미생물에 의한 감염에 취약해지는 상태가 된다. 건강한 장내미생물에 의해 유지되는 “Colonization resistance”가 무너지게 되면 여러 병원성 미생물에 의한 감염에 취약해지게 된다. 먼저 우리는 장내 공생미생물을 이용한 enteric pathogen 에 대한 방어에 대해서 설명할 것이다. (Chapter 1)

비브리오 콜레라 균주는 급성 설사를 동반하여 탈수에 이르게 하는 콜레라를 일으키는 원인 균주로 잘 알려져 있다. 하지만 비브리오 콜레라는

사람한테는 감염이 일어나지만 마우스에서는 감염이 일어나지 않는 특징을 가지고 있다. 마우스 모델이 제대로 확립되어 있지 않다는 점은 콜레라 연구에 있어서 큰 장애물로 작용해왔다. 이에 우리는 먼저 마우스에서 비브리오 콜레라 모델을 확립하고자 하였다. 우리는 여러 항생제를 이용해서 모델을 확립하고자 하였고 처리한 항생제 중 클린다마이신 항생제를 처리하였을 때 효과가 있음을 확인하였다. 클린다마이신을 처리하게 되면 장내 미생물의 변화와 함께 콜레라 감염에 취약해진다 라는 사실을 확인하게 되었다. 클린다마이신은 여러 박테리아 중에서도 혐기성 균주를 선택적으로 죽이는 역할을 하는 항생제이다. 장내 미생물은 여러 혐기성 박테리아로 이루어져 있는데 클린다마이신을 처리하게 되면 장내에 존재하는 많은 미생물이 사라지게 된다. 마우스에 클린다마이신을 처리하였을 때 가장 두드러지게 감소하는 미생물은 박테로이데스 계열의 미생물이 현저하게 사라지며 프로티오박테리아에 속하는 미생물은 증가 되어있음을 확인하였다. 이러한 조건의 마우스에 비브리오 콜레라를 감염시켰더니 감염이 이루어지는 것을 확인할 수 있었다. 이로써 우리는 클린다마이신을 이용한 비브리오 콜레라의 마우스 모델을 확립할 수 있었다. 여기서 우리는 비브리오 콜레라의 감염이 변화된 장내미생물 균총에 의한 것이다 라는 가정하에 클린다마이신이 처리된 장내미생물에서는 비브리오 콜레라의 감염이 잘 이루어 질 것이라고 생각하였다. 이에 클린다마이신이 처리된 마우스의 분변을 무균마우스에 이식하여 비브리오 콜레라의 감염을 확인하였다. 클린다마이신이 처리된 마우스의 분변을 이식한 무균마우스에서만 비브리오 콜레라균의 감염이 이루어지는 것을 확인할 수 있었다. 이로써 비브리오 콜레라의 감염은

장내미생물 균총의 변화로 인해 이루어진 것임을 증명하였다. 여기서 우리는 변화된 장내미생물 중 어떠한 것에 의해 콜레라 균의 감염이 이루어지게 되었는지를 확인하였다. 클린다마이신을 처리하였을 때 가장 크게 변화한 *Bacteroides vulgatus* 가 비브리오 콜레라균의 감염과 연관이 있을 거라는 가설을 세우게 되었다. *B. vulgatus* 가 사라진 환경에서 비브리오 콜레라균의 감염이 일어난 것을 바탕으로 하여, *B. vulgatus* 와 비브리오 콜레라 균 간의 상관관계가 존재할 것이라고 생각하였다. 무균마우스를 이용해서 두 균의 상관관계를 확인하였다. 그 결과 *B. vulgatus* 가 존재할 때 비브리오 콜레라 균의 감염이 억제됨을 확인하였다. 이로써 우리는 클린다마이신을 처리하였을 때 장내미생물 분포가 변하며, 마우스 장내 미생물에 우세하게 존재하는 *B. vulgatus* 의 가장 크게 변화하는 것을 확인할 수 있었다. 이렇게 장내 미생물의 변화가 유도된 상황에서 비브리오 콜레라균의 감염이 일어나는 것을 확인할 수 있었다.

그 다음으로 우리는 변화된 장내 미생물이 어떻게 비브리오 콜레라균의 감염이 일어나는 데에 관여하는지에 대해 알아보았다. 변화된 장내 미생물이 만들어내는 어떠한 환경에 의해 비브리오 콜레라균의 감염이 조절된다고 생각하였고, 이에 우리는 그 환경을 찾아내고자 하였다. 장내미생물에 존재하는 특정 대사체에 의해 장내 환경이 변화되고, 그 때문에 감염이 이루어지는 것이라고 생각하고 대사체에 초점을 맞추게 되었다. 장내 미생물 균총의 변화로 유도된 장내 환경의 변화에 의해서 비브리오 콜레라균의 증식, 우점화가 잘 이루어지는 조건으로 변화하게 되면서 감염에 취약해진다는 사실을 확인하였다.

Chapter 1 에서 장내 감염에 있어서 공생미생물의 중요성에 대해 논의했다면 Chapter 2 에서는 염증성 장질환에 있어서 공생미생물의 중요성에 대해서 다루었다. 염증성 장질환은 만성적으로 장에 염증이 유도되는 질환을 의미한다. 이러한 염증성 장질환은 Ulcerative colitis 와 Crohn's disease 두가지로 나뉘게 되는데, 염증이 유도되는 위치에 따라서 UC 와 CD 로 나뉘게 되는데 둘 다 만성적으로 나타나는 염증성 장질환에 속하게 된다. 염증성 장질환의 치료에는 분변이식술이 많이 이루어진다. 건강한 사람의 장내에 존재하는 미생물을 환자에게 이식해 줌으로써 dysbiosis 상태의 장내미생물을 건강하게 만들어 준다. 분변이식술은 매우 효과적인 치료법이지만 부작용 또한 많이 존재한다. 장내 미생물에 존재하는 다양한 미생물은 우리가 알고 있는 미생물도 있지만 우리가 모르는 미생물 또한 존재하기 때문에 그러한 미생물에 의한 부작용이 존재한다. 이러한 부작용을 줄이기 위해서 우리는 Major Gut Microbes among Korean(MGMK) 라고 부르는 균주 컨소시엄을 만들었다. 우리가 잘 알고 있는 균주를 이용하여 분변이식술을 진행하면 부작용을 줄일 수 있을 것이라고 판단하였다. MGMK 균주들은 한국인에게서 많이 발견되는 균주 중에 많이 연구가 된 균주를 바탕으로 선택되었다. 우리는 이 MGMK 균주를 무균마우스에 이식하여 각각의 균주가 서로 경쟁하여 어떻게 colonization 을 이루는지에 대해 알아보고자 하였다. 그 결과 우리는 *Bacteroides thetaiotaomicron, Bacteroides uniformis, Ruminococcus faecis* 가 굉장히 우세하게 colonization 을 하는 것을 확인하였다. 33일 동안 각각의 균주가 어떻게 colonization 을 이루는지 확인하였는데 균주 이식 후 하루 정도 만에 이 세가지 균주가 우세하게 존재하였으며, 실험 종료

때까지도 우세하게 존재하고 있음을 확인하였다. 우리는 이 세가지 균주를 Strong Intestinal colonizer3 (SIC3) 라고 명명하였다.

우리는 SIC3 를 이용하여, 이 균주들이 염증성 장질환을 완화 시킬 수 있는지에 대해 확인하였다. Dextran sulfate sodium (DSS) 를 마우스에 처리하여 colitis model 을 만들고, SIC3 를 처리하여 증상이 완화되는지 확인하였다. Disease associated index (DAI) 등 몇 가지 지표를 이용해서 SIC3의 효능을 확인한 바, SIC3 를 투여한 그룹에서 유의미하게 증상이 감소되었음을 확인할 수 있었다. 즉 염증성 장질환을 치료하는데 있어서 commensal microbes 인 SIC3 가 유의미하게 작용하였음을 입증할 수 있었다.

종합적으로, chapter 1 에서 다룬 enteric infection 과 공생미생물과의 관계에서 공생미생물에 의해 enteric infection 이 조절될 수 있음을 확인하였다. 또한 chapter 2 에서는 염증성 장질환의 치료에 있어서 공생미생물이 작용할 수 있는 지에 대한 가능성 또한 확인할 수 있었다.

핵심되는 말 : 장내미생물, 염증성 장질환, 비브리오 콜레라, *Bacteroides vulgatus*, *Bacteroides thetaiotaomicron*, *Bacteroides uniformis*, *Ruminococcus faecis*

PUBLICATION LIST

You JS, Yong JH, Kim GH, Moon S, Nam KT, Ryu JH, Yoon MY, Yoon SS. Commensal-derived metabolites govern Vibrio cholerae pathogenesis in host intestine. *Microbiome.* 2019;7(1):132.

You JS, Yoon MY, Yoon SS. A consortium of commensal microbes alleviates diseased symptoms by persistent intestinal colonization. (투고 예정)